
000 REVIVING ERROR CORRECTION IN MODERN DEEP 001 TIME-SERIES FORECASTING 002

003 **Anonymous authors**

004 Paper under double-blind review

009 ABSTRACT

011 Modern deep-learning models have achieved remarkable success in time-series
012 forecasting. Yet, their performance degrades in long-term prediction due to error
013 accumulation in autoregressive inference, where predictions are recursively used
014 as inputs. While classical error correction mechanisms (ECMs) have long been
015 used in statistical methods, their applicability to deep learning models remains
016 limited or ineffective. In this work, we revisit the error accumulation problem
017 in deep time-series forecasting and investigate the role and necessity of ECMs
018 in this new context. We propose a simple, architecture-agnostic error correction
019 model that can be integrated with any existing forecaster without requiring retrain-
020 ing. By explicitly decomposing predictions into trend and seasonal components
021 and training the corrector to adjust each separately, we introduce the Universal
022 Error Corrector with Seasonal-Trend Decomposition (UEC-STD), which signifi-
023 cantly improves correction accuracy and robustness across diverse backbones and
024 datasets. Our findings provide a practical tool for enhancing forecasts while offer-
025 ing new insights into mitigating autoregressive errors in deep time-series models.

026 1 INTRODUCTION

028 Time-series forecasting is essential across numerous industries, including finance, healthcare, en-
029 ergy management, and supply chain optimization. In recent years, deep learning models have sig-
030 nificantly improved the accuracy of time-series forecasting (Wu et al., 2023; Zeng et al., 2023; Wang
031 et al., 2024a;b). They outperform traditional methods on real-world benchmarks by leveraging ad-
032 vanced feature extraction and data-driven representations (Siami-Namini & Namin, 2018; Qiu et al.,
033 2024). Despite these advances, long-term forecasting remains a persistent challenge. One approach
034 is to directly train the model to predict a fixed, large number of future steps in a single forward
035 pass. However, this requires significantly larger models, often exhibits degraded accuracy, and is
036 not scalable to arbitrary prediction lengths. A more flexible alternative is autoregressive inference,
037 which generates future steps sequentially by conditioning on previously predicted values. Yet, this
038 paradigm suffers from compounding errors, as inaccuracies introduced at earlier steps propagate and
039 amplify over time (Moreno-Pino et al., 2023).

040 Error modeling has been studied in traditional time-series forecasting, with classical Error Correc-
041 tion Models (ECMs) addressing long-term relationships by using cointegration and making adjust-
042 ments for deviations from equilibrium, defined as a stable long-run relationship that the system
043 gradually returns to after short-term fluctuations (Hansen, 2003; Barigozzi et al., 2024). Similarly,
044 classic methods like ARIMA, based on autoregressive processes, make forecasts by considering past
045 observations, predictions, and errors (Makridakis & Hibon, 1997). However, classical ECMs differ
046 fundamentally from the error correction needed in deep learning models. They adjust for deviations
047 from equilibrium across multiple time series, making them difficult to apply directly to modern deep
048 learning models, which require the correction of errors arising from internal processing and autore-
049 gressive prediction. While error correction has been explored for specific deep learning models in
050 recent research, solutions often involve predefined error functions to refine predictions (Zhang et al.,
051 2021) or the integration of error correction layers within forecasting pipelines (Liu et al., 2020; Li
052 et al., 2024), necessitating costly joint training of both the correction module and the forecasting
053 model. To our knowledge, *there exists no error correction model (ECM) that reliably improves a*
The absence of such an ECM is potentially due to the already high performance of current forecast-

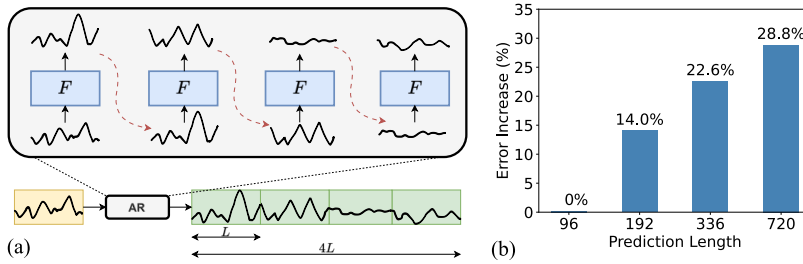


Figure 1: (a) Chunk-based autoregressive (AR) forecasting in time series. Given a forecaster F with a fixed prediction window length L , which equals the input window size, the model’s output must be recursively fed as input to predict a future horizon of length $4L$ (here, using $M = 4$ AR steps). (b) The relative increase in test prediction error when using model-predicted inputs instead of ground-truth, across 4 standard forecasting lengths: 96, 192, 336, and 720. Results are based on TimeMixer with $L = W = 96$ on the ETTh1 dataset.

ing methods, which makes ECMs redundant. Alternatively, it may stem from the risk of overfitting ECMs to specific model or dataset characteristics, thereby hindering their ability to perform well on test data (Nandutu et al., 2022). These considerations give rise to two key research questions under the autoregressive inference setting: (1) Are ECMs necessary for deep learning-based forecasting models? (2) How can ECMs be systematically integrated to generalize and improve the performance of state-of-the-art forecasting architectures?

In this paper, we study the feasibility of integrating ECM into deep forecasters. We propose the *Universal Error Corrector* (UEC), a simple framework that learns correction vectors from the inputs and outputs of pre-trained models. Once trained, UEC adjusts forecasts at inference to mitigate error accumulation over long horizons. While the UEC can be implemented as any machine learning model, we propose a specialized variant for time-series data, the *UEC with Seasonal-Trend Decomposition* (UEC-STD). Time-series forecasts often exhibit distinct long-term trends and short-term seasonal patterns, and the backbone forecaster may struggle differently with each. UEC-STD explicitly separates these components and learns targeted corrections for both, optimizing a weighted loss that balances trend and seasonal errors. The experimental results demonstrate that the UEC-STD consistently reduces error accumulation and significantly improves the accuracy of 3 deep forecasters with minimal additional computational cost. In summary, our contributions are: (i) We pioneer a universal error correction mechanism for modern forecasters without retraining the backbone; (ii) We design UEC-STD, a lightweight plug-in module that explicitly corrects trend and seasonal errors in time-series data; (iii) We validate UEC-STD across diverse datasets and models, showing consistent error reduction, efficiency, and insightful model analyses.

2 METHOD

To begin, we briefly introduce time-series forecasting. Here, the objective is to predict future values of a sequence based on historical observations. Let $\mathcal{D}_{train} = \{X_t\}_{t=1}^{T_{train}}$ represent the observed multivariate time-series data, where $X_t \in \mathbb{R}^D$ is the time-series values at time t , and D is the number of variates. The forecasting task involves predicting future values over a horizon L based on historical time-series observations. Specifically, let the past window of observations be represented as: $X_{t-W+1:t} = \{X_{t-W+1}, X_{t-W+2}, \dots, X_t\}$ where W is the look-back window length. Given this window, we aim to predict the future values of the time-series $X_{t+1}, X_{t+2}, \dots, X_{t+L}$ using a model $F(\cdot)$: $\hat{X}_{t+1:t+L} = F(X_{t-W+1:t})$. The objective is to minimize the forecast error, often defined as the discrepancy between the predicted values $\hat{X}_{t+1:t+L}$ and the true future values $X_{t+1:t+L}$, by minimizing the forecasting loss functions such as MSE or Huber losses (Jadon et al., 2024).

2.1 CHUNK-BASED AUTOREGRESSIVE PREDICTION

Now, we formalize the autoregressive forecasting setup considered in this work. In this approach, during inference, when ground-truth data are unavailable for long-term forecasting, the model feeds

108 its previous predictions back as inputs (Shi et al., 2025). This can cause error propagation, as small
 109 prediction errors accumulate and amplify over time, leading to significant deviations.
 110

111 Formerly, let \hat{X}_t be the predicted value at time t , and X_t the true value. In traditional autoregressive
 112 models, assuming we do not have the true data X_t , the process is: $\hat{X}_{t+1} = F(X_{t-W:t-1} \oplus \hat{X}_t)$
 113 where $X_{t-W:t-1}$ is the history of observations up to time $t-1$, \hat{X}_t is the prediction for step t ,
 114 and \oplus is the concatenation of 2 time-series. In practice, we can apply a chunk-based autoregression
 115 that forecasts a window of L time steps at a time (see Fig. 1 (a)). At the autoregression step
 116 $k = 0, 1, \dots, M$, the predicted chunk $\hat{X}_{t+kL+1:t+(k+1)L}$ is fed back as input for the next prediction:
 117

$$118 \quad \hat{X}_{t+kL+1:t+(k+1)L} = \begin{cases} F(X_{t-W+1:t}) & \text{if } k = 0 \\ F(\hat{X}_{t+kL-W+1:t+kL}) & \text{if } k \geq 1 \end{cases} \quad (1)$$

120 Here, M is the number of autoregressive steps needed to reach the desired horizon length $M \times L$.
 121 From now on, to simplify the notation, we set $\tau = t + kL$ as the chunk boundary at AR step k
 122 starting from timestep t . Here, for any positive index j , if $\tau - W + 1 + j \leq t$:
 123

$$124 \quad \hat{X}_{\tau-W+1+j} = X_{\tau-W+1+j}. \quad (2)$$

125 By optionally using an overlapping window for the final step, chunk-based autoregression allows any
 126 model with a fixed prediction horizon L to produce forecasts of arbitrary length T . For example,
 127 the last autoregressive step reads: $\hat{X}_{t+T-L+1:t+T} = F(\hat{X}_{t+T-L-W+1:t+T-L})$ where $M = \lceil \frac{T}{L} \rceil$ is
 128 the number of chunks and T is the desired forecast length. For convenience, we denote the whole
 129 prediction using AR as:
 130

$$131 \quad \hat{X}_{t+1:t+T} = F_{AR}(X_{t-W:t-1}|T) \quad (3)$$

132 Despite its flexibility, this recursive formulation remains susceptible to error accumulation across
 133 chunks. As seen in Fig. 1 (b), the forecasting error grows with the number of autoregressive steps,
 134 compared to using ground-truth inputs at each step.
 135

2.2 UNIVERSAL ERROR CORRECTION FRAMEWORK

137 **Autoregressive Correction Mechanism** Let $\hat{X}_{t+1:t+L}$ represent the forecasted values, and let
 138 $\Delta\hat{X}_{t+1:t+L}$ be the error correction vector. We propose to compute $\Delta\hat{X}_{t+1:t+L}$ using a neural net-
 139 work, namely Universal Error Corrector (UEC), which is trained to minimize the error between the
 140 corrected values and the ground-truth values. Concretely, the UEC takes the past time-series win-
 141 dows and the forecaster’s predictions as input and computes the error correction vector. First, using
 142 the AR process in Eq. 3, we derive the whole predictions $\hat{X}_{t+1:t+T}$. Next, we iteratively generate
 143 the corrections. Formerly, at $k = 0$:

$$145 \quad \Delta\hat{X}_{t+1:t+L} = \text{UEC}(X_{t-W+1:t}, \hat{X}_{t+1:t+L}) \quad (4)$$

146 For subsequent AR steps ($k \geq 1$), we compute the correction vectors as:
 147

$$148 \quad \Delta\hat{X}_{\tau+1:\tau+L} = \text{UEC}(\hat{X}_{\tau-W+1:\tau}, \hat{X}_{\tau+1:\tau+L}) \quad (5)$$

149 Finally, the whole correction vector $\Delta\hat{X}_{t+1:t+T} = \{\Delta\hat{X}_{t+1}, \Delta\hat{X}_{t+2}, \dots, \Delta\hat{X}_{t+T}\} \in \mathbb{R}^{T \times D}$ is
 150 applied to the forecasted values as follows:
 151

$$152 \quad \hat{X}_{t+j}^{\text{corr}} = \hat{X}_{t+j} + \beta \Delta\hat{X}_{t+j}, \quad \text{for each } j \in [1, T] \quad (6)$$

153 where $\beta \in [0, 1]$ is a scalar hyperparameter that controls the strength of the correction. Setting
 154 $\beta = 0$ disables the correction entirely, while $\beta = 1$ applies full correction.
 155

156 **Training Data Preparation** To train the UEC, we construct supervised training examples where
 157 each sample consists of the input $\in \mathbb{R}^{(W+L) \times D}$ to the UEC and its corresponding ground-truth
 158 output $\in \mathbb{R}^{L \times D}$. To better reflect realistic deployment scenarios where the forecaster F is likely to
 159 produce imperfect predictions, we avoid using the time series used to train F , which may lead to
 160 overfitted predictions and artificially small errors. Instead, we sample from a held-out validation set,
 161 which more accurately represents the model’s generalization behavior.

162 Specifically, we construct training examples for UEC by sampling time series from the validation
 163 dataset $\mathcal{D}_{val} = \{X_t\}_{t=T_{train}}^{T_{train}+T_{val}}$. First, we sample a historical window $X_{t-W+1:t}$ of length W ,
 164 along with a corresponding future window $X_{t+1:t+T'} = \{X_{t+1}, X_{t+2}, \dots, X_{t+T'}\}$, where $T' \geq L$
 165 is a predefined prediction horizon used for training, which can be different than the horizon T during
 166 inference. Then, the forecaster F is used to generate the predictions using AR:
 167

$$\hat{X}_{t+1:t+T'} = F_{AR}(X_{t-W+1:t} | T') \quad (7)$$

169 Next, we sample the ground-truth values $X_{\tau+1:t+(k+1)L} \subseteq X_{t+1:t+T'}$, and compute the ground-
 170 truth correction vector as the error between the predicted and the ground-truth time series:
 171

$$\Delta X_{\tau+1:\tau+L} = X_{\tau+1:\tau+L} - \hat{X}_{\tau+1:\tau+L} \quad (8)$$

172 A training instance for UEC is then a tuple: $\left(\underbrace{(\hat{X}_{\tau-W+1:\tau}, \hat{X}_{\tau+1:\tau+L})}_{\text{input}}, \underbrace{\Delta X_{\tau+1:\tau+L}}_{\text{output}} \right)$
 173
 174
 175
 176
 177

178 **Standard Training Procedure** We split the \mathcal{D}_{val} data into a training set \mathcal{U}_{train} ,
 179 where the UEC is trained by minimizing a correction loss using the Adam opti-
 180 mizer, and a validation set \mathcal{U}_{val} used for early stopping evaluation. At each iter-
 181 ation, we sample tuples $((\hat{X}_{\tau-W+1:\tau}, \hat{X}_{\tau+1:\tau+L}), \Delta X_{\tau+1:\tau+L})$, predict corrections $\Delta \hat{X} =$
 182 $\text{UEC}(\hat{X}_{\tau-W+1:\tau}, \hat{X}_{\tau+1:\tau+L})$, apply them as:
 183

$$\hat{X}_{\tau+1:\tau+L}^{\text{corr}} = \hat{X}_{\tau+1:\tau+L} + \Delta \hat{X}, \quad (9)$$

184 and compute the correction loss:
 185

$$\mathcal{L}_{\text{UEC}} = \frac{1}{L} \sum_{j=1}^L l_{ec}(\hat{X}_{\tau+j}^{\text{corr}}, X_{\tau+j}), \quad (10)$$

186 where l_{ec} can be any regression loss function, such as MSE or Huber loss. Gradients are backprop-
 187 agated only through the UEC, keeping the forecaster fixed.
 188

189 **On Choosing the Correction Strength** To select the correction strength β automatically, we pro-
 190 pose a balanced validation strategy. We use the validation set \mathcal{U}_{val} that is unseen by both the fore-
 191 casters F and the UEC, and randomly sample data from the training set \mathcal{D}_{train} , denoted \mathcal{D}_s , which
 192 the forecaster has seen, such that the combined size satisfies $|\mathcal{U}_{val}| + |\mathcal{D}_s| = |\mathcal{D}_{val}|$, where $|\cdot|$
 193 denotes the number of samples in a dataset. This approach prevents bias in either direction: if β is
 194 tuned only on unseen data, the UEC becomes overly pessimistic about the performance of the fore-
 195 casters F and selects a high correction strength, which can apply excessive adjustments; if tuned only
 196 on seen data, the UEC is too optimistic and selects a low strength. Combining both better reflects
 197 realistic deployment conditions, where the forecaster encounters both familiar and unfamiliar data.
 198 Additionally, we select separate β values depending on the optimization objective: one for MSE and
 199 one for MAE, depending on which metric we aim to optimize for in the backbone forecaster F .
 200

201 2.3 SEASONAL–TREND UEC ARCHITECTURE

202 While the UEC can be instantiated with any prediction model, we design an architecture specialized
 203 for time-series data by explicitly modeling seasonal and trend components.
 204

205 **Seasonal–Trend Decomposition.** Given the UEC input $(\hat{X}_{\tau-W+1:\tau}, \hat{X}_{\tau+1:\tau+L})$, we decompose
 206 the backbone prediction part $\hat{X}_{\tau+1:\tau+L}$ into trend and seasonal components:
 207

$$\hat{X}^t = \text{MA}(\hat{X}_{\tau+1:\tau+L}), \hat{X}^s = \hat{X}_{\tau+1:\tau+L} - \hat{X}^t \quad (11)$$

208 where $\text{MA}(\cdot)$ denotes a moving-average filter. We decompose the backbone prediction into seasonal
 209 and trend components because time-series data usually exhibit both long-term trends and short-term
 210 seasonality. Since the backbone forecaster F may struggle more with one component than the other;
 211 explicitly modeling this structure allows UEC to apply targeted corrections.
 212

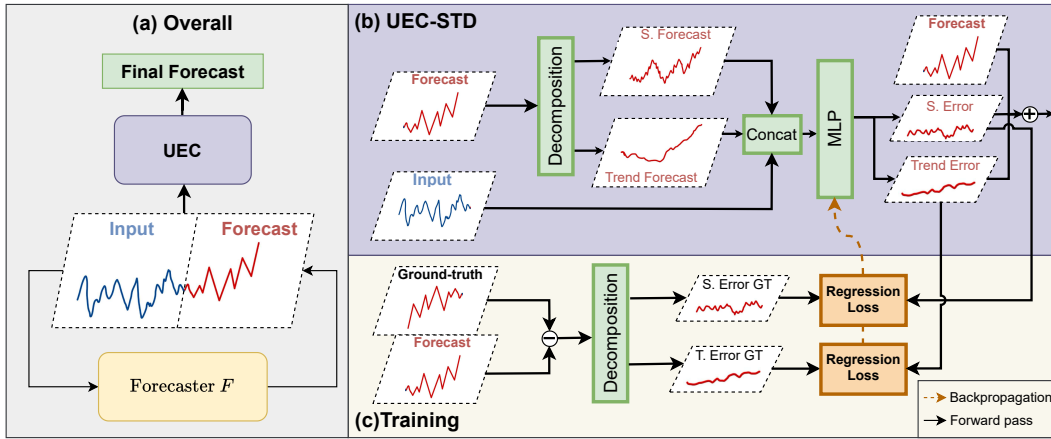


Figure 2: UEC-STD: the corrector refines a pre-trained forecaster by decomposing both the forecast and its error into trend and seasonal components and applying component-wise corrections. (a) *Overall UEC framework*: the corrector takes the input and the forecasted time series from a pre-trained forecaster F , and outputs a corrected forecast. (b) *UEC-STD architecture*: the backbone forecast is decomposed into trend and seasonal components, which are concatenated with historical inputs and fed into an MLP to produce separate correction vectors for trend and seasonality. They are summed with the original forecast to make the final forecast. (c) *Training phase*: the ground-truth error is computed as the difference between the forecast and the true values, then decomposed into trend and seasonal error ground-truth components (T. Error GT and S. Error GT) to supervise the corresponding correction outputs.

Next, we fit \hat{X}^t and \hat{X}^s together with the input $\hat{X}_{\tau-W+1:\tau}$ into a multi-layer perceptron (MLP) to produce seasonal and trend correction vectors:

$$\Delta\hat{X}^t, \Delta\hat{X}^s = \text{FF}_\theta(\hat{X}_{\tau-W+1:\tau}, \hat{X}^t, \hat{X}^s) \quad (12)$$

where FF_θ denotes a feed-forward neural network parameterized by θ , and both outputs $\in \mathbb{R}^{L \times D}$.

Seasonal-Trend Correction. The corrected forecast is reconstructed by adjusting each component and summing:

$$\hat{X}_{\tau+1:\tau+L}^{\text{corr}} = \hat{X}_{\tau+1:\tau+L} + \Delta\hat{X}^t + \Delta\hat{X}^s \quad (13)$$

Seasonal-Trend Training. The corresponding ground truth correction vector $\Delta X_{\tau+1:\tau+L}$ is decomposed into:

$$\Delta X^t = \text{MA}(\Delta X_{\tau+1:\tau+L}), \Delta X^s = \Delta X_{\tau+1:\tau+L} - \Delta X^t \quad (14)$$

The UEC parameters θ are learned by minimizing:

$$\mathcal{L}_{\text{UEC}}^{st} = \lambda_t l_{ec}(\Delta\hat{X}^t, \Delta X^t) + \lambda_s l_{ec}(\Delta\hat{X}^s, \Delta X^s), \quad (15)$$

where λ_t and λ_s control the trade-off between trend and seasonal losses. We refer to this variant as UEC with Seasonal-Trend Decomposition (UEC-STD) to distinguish it from the general UEC.

3 EXPERIMENTAL SETUP

Implementation We conducted experiments using a standard time-series benchmark and codebase¹. Initially, we trained the backbone forecaster using the normal codebase training, with the MSE as the loss function l_{fc} . The specific hyperparameters used for training are consistent with established best practices in the field. For example, we fix the batch size to 128, the learning rate

¹<https://github.com/thuml/Time-Series-Library>

to 0.01, and use the Adam optimizer with default parameters ($\beta_1 = 0.9, \beta_2 = 0.999, \epsilon = 10^{-8}$), and train for 10 epochs with early stopping patience of 10. For further details on the exact parameter settings, we refer the reader to the official codebase. This trained backbone was then used to generate data for the training of the UEC. For UEC, we found that using l_{ec} as the Huber loss led to more stable training for the UEC (see Sec. 4.3), and we therefore adopted it for all subsequent experiments. More details on UEC hyperparameters can be found in Appendix A.

Computing Requirement All experiments are conducted on a single NVIDIA V100 GPU. The training cost of the proposed UEC modules is negligible compared to that of the backbone models. For example, training the TimeMixer backbone on ETTh1 with $L \in [96, 192, 336, 720]$ requires approximately 10 minutes of GPU time, whereas training UEC-STD on that setting takes only about 1 minute, i.e., roughly one-tenth of the backbone training time. This demonstrates that our approach introduces minimal computational overhead while maintaining efficiency.

Evaluation Protocol For each dataset and prediction length L , we (i) train the backbone forecaster on the standard training split (70%) and use the validation split to get the best checkpoint, (ii) train the UEC on the validation split (10%) to correct the backbone, and (iii) report results on the held-out test split (20%). We report average Mean Squared Error (MSE) and Mean Absolute Error (MAE):

$$\text{MSE} = \frac{1}{NLD} \sum_{i=1}^N \sum_{j=1}^L \sum_{d=1}^D (\hat{X}_{t+j,d}^{(i)} - X_{t+j,d}^{(i)})^2, \quad \text{MAE} = \frac{1}{NLD} \sum_{i=1}^N \sum_{j=1}^L \sum_{d=1}^D |\hat{X}_{t+j,d}^{(i)} - X_{t+j,d}^{(i)}|$$

Here N is the number of test segments, L the forecast horizon, and D the dimensionality. We compute metrics per prediction length and then take the mean across lengths.

4 EXPERIMENTAL RESULTS

This section aims to demonstrate the effectiveness of our proposed approach for enhancing autoregressive inference in long-term forecasting. We begin by establishing that autoregressive inference is a strong baseline, warranting further investigation for targeted improvements. We then demonstrate that the limitation of AR can be addressed by integrating UEC into the inference pipeline, resulting in significant performance gains across various backbone forecasters. More specifically, we evaluate multiple design choices for UEC and demonstrate that our proposed UEC-STD architecture consistently achieves the best results across all benchmarks. Finally, we conduct ablation studies and model analyses to assess the contribution of each component in our approach.

4.1 RESULTS ON TIME-SERIES BENCHMARK

AUTOREGRESSION IS A STRONG BASELINE, BUT CORRECTING ITS ERRORS IS NECESSARY

We compare two paradigms for long-term forecasting: (i) **Direct Forecasting (DF)**, which predicts the entire horizon in one pass, and (ii) **Autoregressive (AR)**, which generates predictions iteratively. DF requires horizon-specific models and a higher cost, while AR reuses the same module across steps, making it more efficient and flexible. Experiments on ETTh1, Weather, and Electricity with two backbones (TimeMixer (Wang et al., 2024a) and TimesNet (Wu et al., 2023)) show that AR matches or outperforms DF in 7 of 12 cases (Appendix Table 13), particularly excelling on ETTh1. However, AR suffers from *error accumulation*, where small early mistakes amplify into high MSE/MAE (0.4–0.7) over long horizons, corresponding to up to 28.8% error increase compared to using ground-truth inputs (Fig. 1 (b)). This underscores the need for error correction. Hence, we focus on AR as the main target for correction and omit the DF baseline to save computation.

UEC-STD DELIVERS SUBSTANTIAL AND CONSISTENT IMPROVEMENTS TO AR

The purpose of this experiment section is to evaluate the effectiveness of our proposed UEC in mitigating the errors and improving the overall performance of modern deep forecasting models under autoregressive inference. As such, we examine different UEC architectures on **3 forecasting backbones** (*TimeMixer* (Wang et al., 2024a), *TimesNet* (Wu et al., 2023), and *TimeXer* (Wang et al.,

324
 325 Table 1: Average Error Reduction in MSE compared to backbone for different UEC methods (the
 326 lower the better, negative means improvement). N/A indicates that the method failed to converge or
 327 crashed during training. Bold and underline denote best and second-best results, respectively.

Method	ETTh1	ETTh2	ETTm1	ETTm2	Traffic	Weather	Electricity
AR (No Correction)	0.00	0.00	0.00	0.00	0.00	0.00	0.00
UEC-MLP	0.71	0.05	-0.93	-1.20	-0.67	-1.34	0.17
UEC-Logistic	11.7	5.84	-3.49	0.25	N/A	-3.61	N/A
UEC-Random Forest	1.10	<u>-1.39</u>	-0.92	<u>-1.43</u>	N/A	0.76	N/A
UEC-XGBoost	0.40	-0.46	-11.88	-0.51	N/A	<u>-2.48</u>	N/A
UEC-LSTM	2.48	-0.08	-0.29	24.63	0.36	6.35	-0.52
UEC-GRU	3.49	-0.51	-0.29	4.32	<u>-1.12</u>	4.13	-0.26
UEC-CNN	0.94	-0.77	-0.76	1.96	0.06	4.99	0.04
UEC-Transformer	0.91	-1.22	-0.63	0.47	-0.18	-1.66	-1.19
UEC-STD	-2.39	-1.49	<u>-4.78</u>	-1.78	-1.18	-2.10	<u>-0.91</u>

338
 339
 340 2024b)). They are chosen as efficient and recent strong baselines in time-series long-term fore-
 341 casting. We select **7 datasets** (ETTh1, ETTh2, ETTm1, ETTm2, Electricity, Weather, and Traffic),
 342 which support a long-term prediction horizon up to 720 steps. Moreover, we evaluate **9 different**
 343 **UEC architectures**, ranging from classic machine learning models such as logistic regression and
 344 random forests, to simple neural networks like MLPs and LSTMs, and more sophisticated models
 345 such as Transformers. These architectures follow the standard UEC framework (Sec. 2.2). We
 346 denote these methods as UEC-X, where X refers to the underlying correcting architecture (see Ap-
 347 pendix B). We also include the proposed UEC-STD variant (Sec. 2.3) to validate our special design
 348 for time-series data. All UEC methods apply auto selection of β (Sec. 2.2). To see how UEC helps
 349 the forecasters, we report the error reduction rate (%), Appendix Eq. 18) in MSE and MAE for vari-
 350 ous UEC architectures compared to no correction ($\beta = 0$). The error reduction is then averaged over
 351 3 backbones. Negative values indicate an improvement over the backbone model with no correction,
 352 while positive values denote performance degradation.

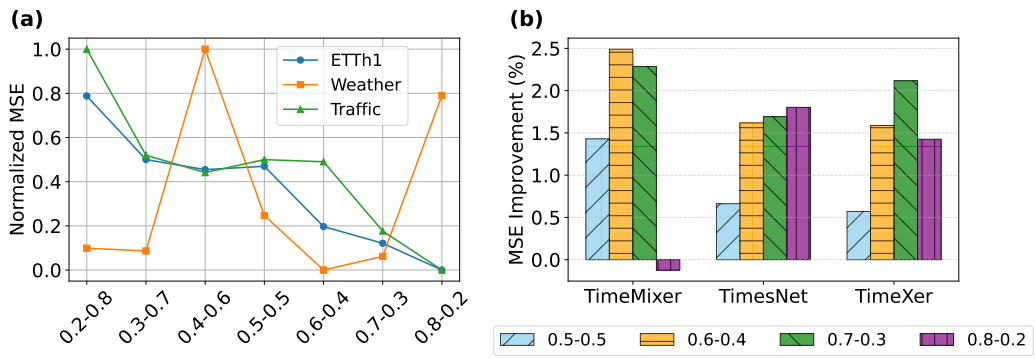
353 Table 1 and Appendix Table 3 summarize the results for improvements in MSE and MAE, respec-
 354 tively. Regarding MSE, overall, most architectures, particularly XGBoost and UEC-STD, achieve
 355 consistent error reductions across multiple datasets. However, some classical machine learning mod-
 356 els, such as XGBoost, Random Forest, and Logistic Regression, fail to scale effectively on large,
 357 high-dimensional datasets like Traffic and Electricity, resulting in training convergence issues de-
 358 spite extensive hyperparameter tuning. Therefore, UEC-STD achieves the best overall performance,
 359 delivering both the greatest average error reduction and the highest consistency across datasets. In
 360 terms of MAE, UEC-STD is the only method that can reliably correct the forecaster’s errors. On
 361 average, across backbones and datasets, **UEC-STD achieves MSE and MAE improvements of**
 362 **2.1% and 0.8%, respectively**, which is comparable to SOTA improvements in the field (Wang
 363 et al., 2024b). Notably, for datasets like ETTm1, UEC-STD attains major error reductions of 4.78%
 364 in MSE and 1.81% in MAE. We provide the details of these experimental results in Appendix C.

364 4.2 ABLATION STUDY ON UEC-STD

366 **Seasonal-Trend Decomposition Components** Here, we compare different design choices for sea-
 367 sonal-trend decomposition (STD) by varying the choice of STD components in UEC input and out-
 368 put (Table 2). We observe that adding trend or seasonal components to inputs only (*No STD Output*)
 369 yields little improvement compared to not using STD at all (*No STD*), with gains of 1.1% MSE on
 370 ETTh1 and 0.4% MSE on Weather, while Traffic shows no change. Modeling STD in UEC output
 371 further improves the performance. In particular, when predicting only seasonal (*No Trend Output*)
 372 or only trend (*No Seasonal Output*), we find that seasonal correction contributes more to ETTh1
 373 (seasonal-only improves MSE by 5.3% vs trend-only 2.7%), whereas both Traffic and Weather ex-
 374 hibit little to no improvement when relying on only one component. Our full setup (*Full*), which uses
 375 both decomposed inputs and predicts separate errors for trend and seasonal components, achieves
 376 the best overall performance, improving MSE/MAE by 5.99%/2.48% on ETTh1, 0.37%/0.30% on
 377 Traffic, and 0.83%/1.45% on Weather compared to the No STD. These demonstrate the complemen-
 378 tary benefits of jointly correcting trend and seasonality, leading to consistent gains across datasets.

378
 379 Table 2: Comparison of different design variants for seasonal–trend decomposition (STD). Each
 380 setting differs in the choice of inputs (raw series \hat{X} , seasonal \hat{X}^s , trend \hat{X}^t) and outputs (predicted
 381 errors $\Delta\hat{X}$, $\Delta\hat{X}^s$, $\Delta\hat{X}^t$). Bold denotes the best results.

382 Setting	383 Input(s)	384 Output(s)	ETTh1	Traffic	Weather
			MSE	MAE	MSE
384 No STD	$\hat{X}_{\tau-W+1:\tau}$	$\Delta\hat{X}$	0.451	0.444	0.545
385 No STD Output	$\hat{X}_{\tau-W+1:\tau}, \hat{X}^t, \hat{X}^s$	$\Delta\hat{X}$	0.446	0.452	0.546
386 No Season Output	$\hat{X}_{\tau-W+1:\tau}, \hat{X}^t, \hat{X}^s$	$\Delta\hat{X}^t$	0.464	0.447	0.544
387 No Trend Output	$\hat{X}_{\tau-W+1:\tau}, \hat{X}^t, \hat{X}^s$	$\Delta\hat{X}^s$	0.427	0.437	0.547
388 Full (Our)	$\hat{X}_{\tau-W+1:\tau}, \hat{X}^t, \hat{X}^s$	$\Delta\hat{X}^t, \Delta\hat{X}^s$	0.424	0.433	0.543
389			0.335	0.239	0.272



400 Figure 3: Seasonal-Trend (ST) Coefficient $\lambda_s - \lambda_t$ analysis. (a) Normalized MSE (0–1) for 3 datasets,
 401 ETTh1, Weather, and Traffic, using TimeMixer across different coefficients; lower values indicate
 402 better performance. (b) Percentage MSE improvement on Weather for three backbones (TimeMixer,
 403 TimesNet, TimeXer) with varying ST coefficients; higher values indicate greater improvement. The
 404 plots show how emphasizing the correction of seasonal and trend affects forecasting performance.

405
 406
 407
 408
 409 **Seasonal-Trend Coefficients** We study different seasonal–trend (ST) coefficient settings $\lambda_s - \lambda_t$
 410 across datasets (ETTh1, Weather, Traffic) and backbones (TimeMixer, TimesNet, TimeXer). In
 411 Fig.3a, we fix $\beta = 0.1$ and vary coefficients from 0.2–0.8 to 0.8–0.2. Results show that higher
 412 seasonal weighting improves accuracy: ETTh1 and Traffic perform best with 0.8–0.2 (1.4%, 0.96%
 413 improvements), while Weather prefers 0.6–0.4 (1.07%). Overweighting seasonality, however, can
 414 hurt datasets dominated by long-term trends. In Fig. 3b, we repeat this analysis for Weather across
 415 backbones. The trend holds broadly: emphasizing seasonality improves accuracy, though the
 416 optimal balance depends on datasets and backbones. Overall, we recommend starting with 0.5–0.5 and
 417 adjusting toward seasonality (e.g., 0.6–0.4 or 0.8–0.2) based on dataset characteristics.

4.3 MODEL ANALYSIS

421 In this section, we analyze the general behavior of the UEC framework. For simplicity and to reduce
 422 the confounding effects of Seasonal–Trend components, we use UEC-MLP as the representative
 423 architecture, while we expect UEC-STD to exhibit better behaviors.

424
 425 **Long-term Correction Behaviors** We present four qualitative cases in Appendix Fig. 4 comparing
 426 predictions *with* and *without* UEC on the *Traffic* dataset (prediction length = 720). Across all
 427 cases, the UEC-enhanced forecasts closely follow the ground truth in level, trend, and oscillation,
 428 whereas the no-UEC baseline exhibits *collapse*, which shows nearly flat, low-variance trajectories
 429 that remain anchored to early forecast values. In general, UEC helps long-horizon rollouts by
 430 adding learned, context-aware residuals to the backbone forecast at each autoregressive step. These
 431 corrections restore amplitude and phase, counter drift, and smooth chunk boundaries, so predictions
 432 maintain appropriate variability and stay aligned with the target signal.

432 **UEC Training Loss** To examine the impact of training loss on UEC performance, we report re-
433 sults using different l_{ec} (Huber, L1, and MSE) in Appendix Table 14. Experiments use ETTh1
434 dataset with 2 backbones: TimeMixer and TimesNet. Overall, Huber loss achieves the lowest aver-
435 age MSE and MAE in four cases, the best among the three losses. While different losses may yield
436 gains in other cases, we adopt Huber loss as the default for training UEC to avoid costly tuning.
437

438
439 **Improvement Gain with Extended Training.** One question is whether UEC’s gains arise from
440 holding out validation data for training the corrector. To test this, we retrain backbones on both train-
441 ing and validation sets (so UEC has no data advantage) and then train UEC on the same validation
442 portion to correct the new backbones. Results on Traffic (Appendix Fig. 6) show UEC still improves
443 performance, confirming the benefits come from learning correction patterns rather than data with-
444 holding. Improvements vary by backbone: weaker models like TimesNet gain more, while stronger
445 ones like TimeMixer benefit less and may even overfit when retrained with extra data. Hence, we
446 recommend training backbones on the original data and reserving validation solely for UEC.
447

448 **5 RELATED WORKS**

449
450 **Classical Error Correction Models** Traditional Error Correction Models (ECMs) are widely used
451 in econometrics (Hansen, 2003; Barigozzi et al., 2024). These models explicitly capture deviations
452 from equilibrium and apply corrective terms to guide predictions back toward the expected state.
453 However, ECMs are designed for linear, low-dimensional systems and rely on statistical assumptions
454 that are difficult to transfer to the complex dynamics of modern deep-learning models. Their reliance
455 on multivariate co-integration prevents their applicability to high-dimensional forecasting scenarios.
456

457
458 **Autoregressive Deep Learning and Error Accumulation** Deep learning models have recently
459 achieved state-of-the-art performance in time-series forecasting (Liu et al., 2023; Zeng et al., 2023;
460 Wang et al., 2024b). TimeMixer (Wang et al., 2024a), a decomposable multiscale mixing frame-
461 work, improves forecasting by separating temporal components and mixing information across mul-
462 tiple scales with high efficiency. TimeMixer++ (Wang et al., 2025) further generalizes this approach
463 by introducing a universal time-series pattern machine that enhances multi-scale modeling across di-
464 verse predictive tasks. DeformableTST (Luo & Wang, 2024) addresses the limitations of traditional
465 transformer patching by incorporating deformable attention, enabling the model to flexibly focus on
466 the most relevant temporal regions without fixed segmentation. Cross-series relational models like
467 TimeBridge (Liu et al., 2025) learn dependencies among correlated time series through inter-series
468 attention, leveraging shared patterns to improve multivariate forecasting performance. Despite the
469 advances, these models often train with fixed input-output lengths, and to predict longer horizons,
470 they must rely on autoregressive decoding: using the prediction as the input for the next forecasting
471 step. Unfortunately, this recursive strategy leads to unavoidable compounding errors over longer
472 horizons (Moreno-Pino et al., 2023). A temporary workaround is to train separate models for differ-
473 ent prediction lengths. While this can help manage error accumulation, it incurs additional training
474 time, storage, and complexity costs. Thus, it is not suited for ultra-long or unknown inference
475 lengths, limiting its scalability and practical applicability.
476

477 **Error Correction in Deep Learning for Time-Series Forecasting** . Recent studies have explored
478 incorporating error correction mechanisms using deep learning to improve time-series forecasting
479 accuracy. Liu et al. (2020) propose modules that explicitly learn residual errors during training,
480 while Zhang et al. (2021) refine predictions using predefined loss-based error functions. Others
481 attempt to learn the error correction function, such as using LSTMs to model the residuals of clas-
482 sical ARIMA forecasts (Nandutu et al., 2022) or (Li et al., 2024), jointly training the forecasting
483 model with a diffusion process to refine its predictions. While promising, these methods are often
484 tied to specific architectures or training pipelines, limiting their generality. To date, no architecture-
485 agnostic error correction approach consistently improves modern forecasters. This work is the first
to address this gap by proposing a general and modular solution.

486 6 CONCLUSION 487

488 In this paper, we revisited the problem of error accumulation in deep autoregressive time-series
489 forecasting and proposed a simple, architecture-agnostic error correction mechanism that can be
490 integrated with any existing deep learning forecaster without retraining. Our proposed approach,
491 named Universal Error Correcter with Seasonal-Trend Decomposition (UEC-STD), consistently im-
492 proves long-term prediction accuracy across multiple benchmarks and backbone models, providing
493 both practical utility and novel insights into autoregressive error mitigation. While effective, our
494 method introduces a modest computational overhead due to the additional error correction prediction.
495 Future work will focus on designing more efficient UEC variants that minimize computational
496 overhead without compromising performance. Moreover, investigating adaptive correction mech-
497 anisms and extending our evaluation to diverse real-world scenarios, such as multi-modality and
498 irregularly sampled time series, offers promising avenues to improve the robustness and scalability
499 of deep time-series forecasting.

500 501 REPRODUCIBILITY STATEMENT 502

503 Details of implementations and experiments can be found in the Appendix. Upon publication,
504 we will release the implementation as open-source with the necessary instructions to ensure re-
505 producibility.

506 507 LLM USAGE 508

509 Large Language Models (LLMs) were not involved in the design, implementation, or analysis of
510 our method. They were only used to refine the presentation of the paper by correcting grammar and
511 improving writing clarity.

513 REFERENCES 514

515 Matteo Barigozzi, Giuseppe Cavaliere, and Lorenzo Trapani and. Inference in heavy-tailed nonsta-
516 tionary multivariate time series. *Journal of the American Statistical Association*, 119(545):565–
517 581, 2024. doi: 10.1080/01621459.2022.2128807. URL <https://doi.org/10.1080/01621459.2022.2128807>.

519 Tianqi Chen and Carlos Guestrin. Xgboost: A scalable tree boosting system. In *Proceedings of the*
520 *22nd acm sigkdd international conference on knowledge discovery and data mining*, pp. 785–794,
521 2016.

522 Peter Reinhard Hansen. Structural changes in the cointegrated vector autoregressive model.
523 *Journal of Econometrics*, 114(2):261–295, 2003. ISSN 0304-4076. doi: [https://doi.org/10.1016/S0304-4076\(03\)00085-X](https://doi.org/10.1016/S0304-4076(03)00085-X). URL <https://www.sciencedirect.com/science/article/pii/S030440760300085X>.

527 Aryan Jadon, Avinash Patil, and Shruti Jadon. A comprehensive survey of regression-based loss
528 functions for time series forecasting. In *International Conference on Data Management, Analytics
& Innovation*, pp. 117–147. Springer, 2024.

530 Yuxin Li, Wenchao Chen, Xinyue Hu, Bo Chen, baolin sun, and Mingyuan Zhou. Transformer-
531 modulated diffusion models for probabilistic multivariate time series forecasting. In *The Twelfth
532 International Conference on Learning Representations*, 2024. URL <https://openreview.net/forum?id=qae04YACHs>.

534 Peiyuan Liu, Beiliang Wu, Yifan Hu, Naiqi Li, Tao Dai, Jigang Bao, and Shu-Tao Xia. Timebridge:
535 Non-stationarity matters for long-term time series forecasting. *International Conference on Ma-
536 chine Learning*, 2025.

538 Yong Liu, Tengge Hu, Haoran Zhang, Haixu Wu, Shiyu Wang, Lintao Ma, and Mingsheng Long.
539 itransformer: Inverted transformers are effective for time series forecasting. In *The Twelfth Inter-
national Conference on Learning Representations*, 2023.

540 Yuxuan Liu, Jiangyong Duan, and Juan Meng. Difference attention based error correction lstm
541 model for time series prediction. In *Journal of Physics: Conference Series*, volume 1550, pp.
542 032121. IOP Publishing, 2020.

543

544 Donghao Luo and Xue Wang. DeformableTST: Transformer for time series forecasting without
545 over-reliance on patching. In *The Thirty-eighth Annual Conference on Neural Information Pro-*
546 *cessing Systems*, 2024.

547

548 Spyros Makridakis and Michele Hibon. Arma models and the box-jenkins methodology. *Journal*
549 *of forecasting*, 16(3):147–163, 1997.

550

551 Fernando Moreno-Pino, Pablo M. Olmos, and Antonio Artés-Rodríguez. Deep autoregressive
552 models with spectral attention. *Pattern Recognition*, 133:109014, 2023. ISSN 0031-3203.
553 doi: <https://doi.org/10.1016/j.patcog.2022.109014>. URL <https://www.sciencedirect.com/science/article/pii/S0031320322004940>.

554

555 Irene Nandutu, Marcellin Atemkeng, Nokubonga Mgqatsa, Sakayo Toadoum Sari, Patrice Okouma,
556 Rockefeller Rockefeller, Theophilus Ansah-Narh, Jean Louis Ebongue Kedieng Fendji, and
557 Franklin Tchakounte. Error correction based deep neural networks for modeling and predicting
558 south african wildlife–vehicle collision data. *Mathematics*, 10(21), 2022. ISSN 2227-7390. doi:
559 [10.3390/math10213988](https://doi.org/10.3390/math10213988). URL <https://www.mdpi.com/2227-7390/10/21/3988>.

560

561 F. Pedregosa, G. Varoquaux, A. Gramfort, V. Michel, B. Thirion, O. Grisel, M. Blondel, P. Pretten-
562 hofer, R. Weiss, V. Dubourg, J. Vanderplas, A. Passos, D. Cournapeau, M. Brucher, M. Perrot, and
563 E. Duchesnay. Scikit-learn: Machine learning in Python. *Journal of Machine Learning Research*,
12:2825–2830, 2011.

564

565 Xiangfei Qiu, Jilin Hu, Lekui Zhou, Xingjian Wu, Junyang Du, Buang Zhang, Chenjuan Guo,
566 Aoying Zhou, Christian S Jensen, Zhenli Sheng, et al. Tfb: Towards comprehensive and fair
567 benchmarking of time series forecasting methods. *Proceedings of the VLDB Endowment*, 17(9):
568 2363–2377, 2024.

569

570 Xiaoming Shi, Shiyu Wang, Yuqi Nie, Dianqi Li, Zhou Ye, Qingsong Wen, and Ming Jin. Time-
571 moe: Billion-scale time series foundation models with mixture of experts. In *The Thirteenth*
572 *International Conference on Learning Representations*, 2025. URL <https://openreview.net/forum?id=e1wDDFmlVu>.

573

574 Sima Siami-Namini and Akbar Siami Namin. Forecasting economics and financial time series:
575 Arima vs. lstm. *arXiv preprint arXiv:1803.06386*, 2018.

576

577 Shiyu Wang, Haixu Wu, Xiaoming Shi, Tengge Hu, Huakun Luo, Lintao Ma, James Y Zhang,
578 and Jun Zhou. Timemixer: Decomposable multiscale mixing for time series forecasting. *arXiv*
579 *preprint arXiv:2405.14616*, 2024a.

580

581 Shiyu Wang, Jiawei LI, Xiaoming Shi, Zhou Ye, Baichuan Mo, Wenze Lin, Ju Shengtong, Zhixuan
582 Chu, and Ming Jin. Timemixer++: A general time series pattern machine for universal predictive
583 analysis. In *The Thirteenth International Conference on Learning Representations*, 2025. URL
584 <https://openreview.net/forum?id=1CLzLXSFNn>.

585

586 Yuxuan Wang, Haixu Wu, Jiaxiang Dong, Guo Qin, Haoran Zhang, Yong Liu, Yunzhong Qiu, Jian-
587 min Wang, and Mingsheng Long. Timexer: Empowering transformers for time series forecasting
588 with exogenous variables. In *The Thirty-eighth Annual Conference on Neural Information Pro-*
589 *cessing Systems*, 2024b.

590

591 Haixu Wu, Tengge Hu, Yong Liu, Hang Zhou, Jianmin Wang, and Mingsheng Long. Timesnet:
592 Temporal 2d-variation modeling for general time series analysis. In *The Eleventh International*
593 *Conference on Learning Representations*, 2023.

594

595 Ailing Zeng, Muxi Chen, Lei Zhang, and Qiang Xu. Are transformers effective for time series
596 forecasting? In *Proceedings of the AAAI conference on artificial intelligence*, volume 37, pp.
597 11121–11128, 2023.

594 Shuai Zhang, Yong Chen, Wenyu Zhang, and Ruijun Feng. A novel ensemble deep learning model
595 with dynamic error correction and multi-objective ensemble pruning for time series forecasting.
596 *Information Sciences*, 544:427–445, 2021. ISSN 0020-0255. doi: <https://doi.org/10.1016/j.ins.2020.08.053>. URL <https://www.sciencedirect.com/science/article/pii/S0020025520308197>.

599
600
601
602
603
604
605
606
607
608
609
610
611
612
613
614
615
616
617
618
619
620
621
622
623
624
625
626
627
628
629
630
631
632
633
634
635
636
637
638
639
640
641
642
643
644
645
646
647

648 APPENDIX
649

650 A DETAILS ON UEC-STD IMPLEMENTATIONS 651

652 A.1 TRAINING AND EVALUATION SUMMARY 653

654 For each dataset and prediction length L , the training and evaluation process consists of four stages:
655

656 1. **Backbone training.** The forecaster F is trained on the training split \mathcal{D}_{train} (70%), and the
657 best checkpoint is selected based on performance on the validation split \mathcal{D}_{val} (10%).
658 2. **UEC-STD training.** Supervised seasonal and trend correction data (\mathcal{U}_{train} and \mathcal{U}_{val}) is
659 derived from the validation split \mathcal{D}_{val} , where 70% is used for training and 30% is reserved
660 for early stopping and tuning the correction strength β . The UEC-STD is then trained
661 following the procedure described in Sect. 2.2 and Sect. 2.3, using 100 training steps with
662 a batch size of 64.
663 3. **Correction strength selection.** The correction weight $\beta \in [0, 1]$ is tuned automatically
664 using the validation strategy described in Sect. 2.2.
665 4. **Evaluation.** The trained UEC-STD is applied autoregressively to backbone forecasts, and
666 corrected predictions are generated according to Eq. 6. Final performance is reported on
667 the held-out test split (20%).
668

669 A.2 SEASONAL-TREND MOVING AVERAGE DECOMPOSITION. 670

671 We decompose the backbone forecast $\hat{X}_{\tau+1:\tau+L}$ into trend and seasonal components using moving
672 average decomposition:
673

674
$$\hat{X}^t = \text{MA}(\hat{X}_{\tau+1:\tau+L}), \quad \hat{X}^s = \hat{X}_{\tau+1:\tau+L} - \hat{X}^t, \quad (16)$$
675

676 where $\text{MA}(\cdot)$ is a 1D convolution-based centred moving average (default kernel size $ks = 25$),
677 computed as in Algorithm 1.
678

679 **Algorithm 1** 1D Moving-Average Trend Computation
680

681 1: **Input:** $\hat{X}_{\tau+1:\tau+L}$, kernel size ks (odd, default 25)
682 2: **Output:** Trend component of $\hat{X}_{\tau+1:\tau+L}$, same shape
683 3: $pad \leftarrow (ks - 1)/2$
684 4: $filt \leftarrow 1D$ averaging filter of length ks with values $1/ks$
685 5: $\hat{X}^t \leftarrow \text{conv1d}(\hat{X}_{\tau+1:\tau+L}, filt, padding = pad)$
686 6: **Return** \hat{X}^t

687 Next, we fit \hat{X}^t and \hat{X}^s together with the input $\hat{X}_{\tau-W+1:\tau}$ into a multi-layer perceptron (MLP) to
688 produce seasonal and trend correction vectors:
689

690
$$\hat{\Delta}X^t, \hat{\Delta}X^s = \text{FF}_\theta(\hat{X}_{\tau-W+1:\tau}, \hat{X}^t, \hat{X}^s) \quad (17)$$
691

692 A.3 MODEL ARCHITECTURE 693

694 FF_θ is a lightweight two-stage MLP designed to refine base predictions by modeling seasonal and
695 trend errors. Assuming an input tensor $x \in \mathbb{R}^{B \times T \times D}$, it will be processed as follows.
696

697 Before entering Subnetwork 1, the input x is reshaped to $(B \times D, T)$ so that each feature dimension
698 can be processed independently along the temporal axis. Subnetwork 1 applies a two-layer MLP
699 with ReLU activation and dropout to capture temporal dependencies in a parameter-efficient manner:
700

701 **Subnetwork 1:**

$$h = \text{Dropout}(W_2 \sigma(W_1 x)),$$

702 where $W_1 \in \mathbb{R}^{T \times H}$, $W_2 \in \mathbb{R}^{H \times T}$, σ denotes the ReLU activation, and H is the hidden size (default
703 $H = 32$). This design allows the model to capture temporal dependencies in a parameter-efficient
704 manner while using dropout value of 0.5 for regularization.

705 The output of Subnetwork 1 is then permuted back to (B, T, D) before entering Subnetwork 2. This
706 second subnetwork is a two-layer MLP, which is responsible for aggregating feature information
707 and projecting into the output space:

709 **Subnetwork 2:**

$$y = \text{Dropout}(W_4 \sigma(W_3 h)),$$

711 where $W_3 \in \mathbb{R}^{D \times H}$ and $W_4 \in \mathbb{R}^{H \times D}$. We then split y into $y_{\text{trend}} = \hat{\Delta}X^t$ and $y_{\text{seasonal}} = \hat{\Delta}X^s$
712 where both $y_{\text{trend}}, y_{\text{seasonal}} \in \mathbb{R}^{B \times L \times D}$. These components are subsequently used in Eq. 13 to
713 compute the final correction value.

715 **B DETAILS ON BASELINE IMPLEMENTATIONS**

717 We implement a diverse set of baseline error correctors spanning traditional machine learning ap-
718 proaches and modern neural architectures. Throughout, each of these UEC models takes the input
719 sequence $x = (\hat{X}_{\tau-W+1:\tau}, \hat{X}_{\tau+1:\tau+L})$ where $x \in \mathbb{R}^{B \times T \times D}$ and outputs $y = \Delta\hat{X}_{\tau+1:\tau+L}$ where
720 $y \in \mathbb{R}^{B \times L \times D}$. These baseline correctors were also trained on the correction data constructed from
721 the validation split \mathcal{D}_{val} , similar to our proposed UEC-STD.

723 **B.1 TRADITIONAL MODELS**

725 **UEC-Logistic.** We implement a logistic regression model using `scikit-learn`'s pipeline (Pe-
726 dregosa et al., 2011), which combines feature scaling, PCA, and a ridge regression head. Specif-
727 ically, x is flattened into $(B, T \times D)$, normalized via `StandardScaler`, reduced using PCA to
728 retain 95% of variance, and finally fitted with a ridge regressor using the SAG solver to predict
729 flattened targets $(B, L \times D)$. The predicted output is then reshaped back to (B, L, D) to match the
730 original temporal and feature dimensions.

731 **UEC-Random Forest.** A random forest regressor using `scikit-learn` (Pedregosa et al., 2011)
732 is trained on flattened features $(B, T \times D)$ to predict flattened targets $(B, L \times D)$. We use 20 trees
733 with a maximum depth of 6. The predicted outputs are reshaped back to (B, L, D) to recover the
734 original temporal structure.

736 **UEC-XGBoost.** We implement an XGBoost regressor with GPU acceleration
737 (`tree_method=gpu_hist, device=cuda`) using `dmlc xgboost.XGB` (Chen & Guestrin,
738 2016). Similar to Random Forest, x is flattened into $(B, T \times D)$. The default configuration uses 20
739 boosting rounds, maximum depth 6, learning rate 0.3, and subsample ratio 1.0. After prediction,
740 outputs are reshaped from $(B, L \times D)$ back to (B, L, D) to maintain consistency with the input
741 dimensions.

742 **B.2 NEURAL MODELS**

744 **UEC-MLP.** As a simple neural baseline, we uses the same architecture as described in Sect. A.3,
745 but directly takes the original forecast $\hat{X}_{\tau+1:\tau+L}$ as input without decomposing it into trend and
746 seasonal components.

748 **UEC-LSTM & UEC-GRU.** We implement both GRU- and LSTM-based recurrent correctors.
749 Given $x \in \mathbb{R}^{B \times T \times D}$, the sequence is passed through an RNN encoder (hidden dimension 32,
750 configurable layers, dropout 0.5). The hidden outputs (B, T, H) are projected through a two-layer
751 MLP with ReLU activations and dropout to produce (B, L, D) .

752 **UEC-CNN.** We apply 1D temporal convolutions to capture local dependencies in the sequence.
753 The input x is permuted to (B, D, T) and processed by two convolutional layers (kernel size 3,
754 hidden dimension 32), followed by dropout. The output is projected with a two-layer MLP into
755 (B, L, D) .

756 **UEC-Transformer.** We use a transformer encoder with learnable positional embeddings. The
757 input x is first projected into a hidden space (64 dimensions), added with positional encodings, and
758 passed through a stack of 2 encoder layers with 4 attention heads and feedforward dimension 128.
759 The outputs are mapped via a two-layer MLP with ReLU and dropout to (B, L, D) .
760

761 **B.3 TRAINING SETUP**
762

763 Each baseline is evaluated under the same autoregressive correction setting as our proposed model
764 for fair comparison.
765

766 **C DETAILS ON EXPERIMENTAL RESULTS**
767

768 **C.1 EVALUATION METRIC**
769

770 The reduction is calculated as:
771

$$\text{Error Reduction} = \frac{\text{MSE/MAE}_{\text{UEC}} - \text{MSE/MAE}_{\text{Backbone}}}{\text{MSE/MAE}_{\text{Backbone}}} \times 100\% \quad (18)$$

774 **C.2 AVERAGE MAE REDUCTION ACROSS MODELS**
775

776 Table 3 reports the average error reduction in MAE compared to the backbone for different UEC
777 methods. Negative values indicate improvements, while positive values denote error increases. N/A
778 indicates that the method failed to converge or crashed during training. Bold and underline denote
779 best and second-best results, respectively.
780

781 Table 3: Average Error Reduction in MAE compared to backbone for different UEC methods (the
782 lower the better, negative means improvement). N/A indicates that the method failed to converge or
783 crashed during training. Bold and underline denote best and second-best results, respectively.
784

Method	ETTh1	ETTh2	ETTm1	ETTm2	Traffic	Weather	Electricity
AR (No Correction)	0.00	0.00	0.00	0.00	0.00	0.00	0.00
UEC-MLP	0.01	0.21	-0.48	-0.31	<u>-1.09</u>	2.20	-0.08
UEC-Logistic	0.91	9.06	-0.97	1.02	N/A	2.54	N/A
UEC-Random Forest	-0.74	<u>-0.48</u>	-1.27	-1.05	N/A	3.51	N/A
UEC-XGBoost	<u>-0.47</u>	0.85	-5.72	0.42	N/A	4.01	N/A
UEC-LSTM	2.25	0.13	-0.20	14.5	-1.70	3.72	-0.48
UEC-GRU	3.53	0.30	-0.26	3.05	-1.53	3.04	-0.32
UEC-CNN	1.99	-0.33	0.17	1.19	-0.43	1.24	-0.13
UEC-Transformer	0.90	-0.24	-0.39	7.45	-0.82	1.39	-1.09
UEC-STD	-0.44	-0.50	<u>-1.81</u>	<u>-0.50</u>	-0.89	-0.83	<u>-0.85</u>

795
796
797
798
799
800
801
802
803
804
805
806
807
808
809

810 C.3 RAW MSE AND MAE RESULTS

812 Table 4, Table 5 and Table 7 report the raw MSE and MAE results for all compared methods under
 813 the TimeMixer, TimesNet and TimeXer backbones, respectively. For each dataset and prediction
 814 horizon, the best and second-best values are highlighted in red and blue. The bottom rows further
 815 summarize the number of times each method achieved the best or second-best performance across
 816 all settings. These results form the basis for the error-reduction analyses in the main text and clearly
 817 demonstrate that our proposed UEC-STD consistently delivers the best overall performance.

818
 819 Table 4: Raw MSE and MAE results using TimeMixer as the backbone forecaster across multiple
 820 datasets and horizons. Lower values are better. Red denotes the best value and blue is the second
 821 best.

Dataset	STD (Ours)		MLP		Logistic		RF		XGB		LSTM		GRU		CNN		TF		TimeMixer		
	MSE	MAE	MSE	MAE	MSE	MAE	MSE	MAE	MSE	MAE	MSE	MAE	MSE	MAE	MSE	MAE	MSE	MAE	MSE	MAE	
ETTh1	96	0.370	0.399	0.393	0.407	0.381	0.402	0.392	0.3400	0.388	0.397	0.378	0.404	0.383	0.426	0.376	0.408	0.387	0.408	0.377	0.397
	192	0.414	0.425	0.440	0.436	0.427	0.430	0.437	0.428	0.433	0.426	0.428	0.432	0.433	0.454	0.424	0.436	0.437	0.437	0.427	0.427
	336	0.449	0.444	0.475	0.456	0.464	0.451	0.470	0.448	0.469	0.447	0.470	0.455	0.473	0.475	0.462	0.458	0.479	0.459	0.465	0.449
	720	0.463	0.463	0.496	0.496	0.480	0.470	0.476	0.464	0.484	0.464	0.482	0.475	0.491	0.499	0.475	0.481	0.500	0.480	0.474	0.466
	Avg	0.424	0.433	0.451	0.445	0.438	0.438	0.444	0.420	0.444	0.434	0.440	0.442	0.445	0.464	0.434	0.446	0.451	0.459	0.435	0.434
ETTh2	96	0.292	0.343	0.293	0.344	0.326	0.399	0.290	0.343	0.294	0.350	0.296	0.346	0.293	0.347	0.294	0.344	0.291	0.344	0.293	0.343
	192	0.374	0.395	0.377	0.396	0.410	0.447	0.371	0.394	0.375	0.400	0.377	0.396	0.373	0.397	0.377	0.395	0.371	0.394	0.376	0.395
	336	0.427	0.437	0.431	0.440	0.463	0.487	0.422	0.435	0.428	0.443	0.428	0.439	0.424	0.439	0.430	0.438	0.422	0.436	0.428	0.438
	720	0.510	0.492	0.513	0.496	0.556	0.540	0.497	0.485	0.508	0.495	0.512	0.496	0.507	0.494	0.504	0.490	0.499	0.488	0.510	0.493
	Avg	0.401	0.416	0.404	0.419	0.439	0.468	0.395	0.414	0.401	0.422	0.403	0.419	0.399	0.419	0.401	0.417	0.396	0.416	0.402	0.417
ETTm1	96	0.318	0.362	0.325	0.360	0.322	0.360	0.326	0.361	0.321	0.361	0.327	0.362	0.328	0.362	0.326	0.367	0.291	0.344	0.293	0.343
	192	0.374	0.396	0.385	0.397	0.379	0.396	0.385	0.399	0.378	0.397	0.387	0.399	0.386	0.400	0.386	0.403	0.388	0.400	0.388	0.400
	336	0.425	0.428	0.440	0.432	0.433	0.431	0.440	0.434	0.431	0.431	0.442	0.434	0.443	0.435	0.440	0.437	0.443	0.435	0.443	0.436
	720	0.546	0.484	0.568	0.492	0.558	0.591	0.569	0.495	0.554	0.490	0.573	0.495	0.575	0.495	0.570	0.496	0.573	0.496	0.575	0.498
	Avg	0.416	0.418	0.430	0.420	0.423	0.445	0.430	0.422	0.421	0.420	0.432	0.423	0.434	0.423	0.431	0.426	0.424	0.419	0.423	0.419
ETTm2	96	0.174	0.259	0.174	0.258	0.173	0.267	0.171	0.259	0.173	0.266	0.185	0.276	0.185	0.276	0.202	0.289	0.175	0.258	0.176	0.258
	192	0.242	0.303	0.243	0.303	0.238	0.308	0.235	0.302	0.237	0.308	0.253	0.321	0.253	0.321	0.267	0.330	0.242	0.303	0.245	0.304
	336	0.310	0.345	0.312	0.347	0.303	0.350	0.299	0.344	0.304	0.349	0.321	0.364	0.331	0.370	0.310	0.347	0.316	0.349	0.312	0.349
	720	0.419	0.408	0.422	0.411	0.407	0.410	0.405	0.406	0.405	0.410	0.427	0.424	0.427	0.424	0.431	0.427	0.418	0.410	0.427	0.413
	Avg	0.288	0.328	0.288	0.329	0.280	0.334	0.278	0.327	0.279	0.334	0.322	0.346	0.322	0.346	0.308	0.342	0.286	0.329	0.290	0.329
Traffic	96	0.477	0.310	0.478	0.310	N/A	N/A	N/A	N/A	N/A	N/A	0.476	0.308	0.477	0.309	0.480	0.311	0.481	0.311	0.481	0.312
	192	0.514	0.323	0.515	0.322	N/A	N/A	N/A	N/A	N/A	N/A	0.513	0.320	0.513	0.321	0.518	0.324	0.519	0.324	0.518	0.325
	336	0.554	0.337	0.556	0.337	N/A	N/A	N/A	N/A	N/A	N/A	0.552	0.335	0.553	0.336	0.560	0.340	0.560	0.340	0.560	0.340
	720	0.627	0.372	0.631	0.374	N/A	N/A	N/A	N/A	N/A	N/A	0.626	0.371	0.627	0.372	0.635	0.376	0.635	0.376	0.635	0.377
	Avg	0.544	0.336	0.545	0.336	N/A	N/A	N/A	N/A	N/A	N/A	0.567	0.334	0.542	0.334	0.548	0.338	0.549	0.338	0.549	0.339
Weather	96	0.158	0.209	0.162	0.217	0.159	0.218	0.159	0.210	0.158	0.216	0.160	0.209	0.160	0.209	0.160	0.209	0.160	0.209	0.161	0.207
	192	0.203	0.251	0.208	0.257	0.203	0.257	0.206	0.252	0.203	0.256	0.207	0.251	0.206	0.251	0.207	0.252	0.206	0.252	0.209	0.250
	336	0.256	0.290	0.262	0.296	0.256	0.294	0.261	0.292	0.257	0.296	0.262	0.291	0.262	0.291	0.263	0.292	0.261	0.292	0.265	0.292
	720	0.338	0.343	0.341	0.346	0.333	0.344	0.340	0.343	0.334	0.346	0.340	0.342	0.342	0.343	0.344	0.344	0.340	0.344	0.348	0.345
	Avg	0.239	0.273	0.243	0.279	0.238	0.278	0.242	0.274	0.238	0.278	0.242	0.273	0.242	0.273	0.244	0.274	0.242	0.274	0.246	0.274
Electricity	96	0.156	0.248	0.157	0.247	N/A	N/A	N/A	N/A	N/A	N/A	0.156	0.247	0.156	0.247	0.156	0.248	0.156	0.247	0.156	0.247
	192	0.177	0.268	0.178	0.267	N/A	N/A	N/A	N/A	N/A	N/A	0.177	0.267	0.177	0.267	0.177	0.268	0.177	0.268	0.177	0.268
	336	0.205	0.293	0.206	0.293	N/A	N/A	N/A	N/A	N/A	N/A	0.203	0.292	0.204	0.293	0.205	0.294	0.205	0.292	0.205	0.294
	720	0.270	0.346	0.271	0.346	N/A	N/A	N/A	N/A	N/A	N/A	0.267	0.343	0.269	0.344	0.271	0.346	0.270	0.345	0.271	0.346
	Avg	0.202	0.289	0.203	0.288	N/A	N/A	N/A	N/A	N/A	N/A	0.201	0.288	0.202	0.288	0.202	0.288	0.202	0.288	0.202	0.289
Best		2	2	0	1	1	0	2	3	1	0	1	3	1	2	0	1	1	0	1	0
Second Best		3	4	0	1	0	0	0	0	2	0	0	0	1	0	2	0	2	2	1	1
Total		5	7	0	2	1	0	2	3	1	0	1	3	2	2	1	2	3	1	1	1

864
865
866
867
868
869
870
871
872
873
874
875
876

877 Table 5: Raw MSE and MAE results using TimesNet as the backbone forecaster across multiple
878 datasets and horizons. Lower values are better. Red denotes the best value and blue is the second
879 best.

Dataset	STD (Ours)		MLP		Logistic		RF		XGB		LSTM		GRU		CNN		TF		TimesNet		
	MSE	MAE	MSE	MAE	MSE	MAE	MSE	MAE	MSE	MAE	MSE	MAE	MSE	MAE	MSE	MAE	MSE	MAE	MSE	MAE	
ETTh1	96	0.423	0.429	0.437	0.442	0.504	0.436	0.446	0.430	0.426	0.430	0.452	0.453	0.436	0.436	0.437	0.447	0.428	0.432	0.428	0.433
	192	0.451	0.448	0.470	0.459	0.533	0.458	0.477	0.452	0.458	0.452	0.490	0.474	0.461	0.455	0.473	0.470	0.464	0.454	0.467	0.458
	336	0.469	0.462	0.490	0.471	0.557	0.477	0.499	0.468	0.480	0.470	0.520	0.493	0.481	0.472	0.500	0.490	0.491	0.473	0.494	0.478
	720	0.481	0.478	0.491	0.486	0.576	0.496	0.500	0.480	0.487	0.488	0.531	0.509	0.493	0.493	0.516	0.516	0.501	0.493	0.501	0.497
	Avg	0.456	0.454	0.472	0.465	0.543	0.466	0.480	0.458	0.463	0.455	0.498	0.482	0.468	0.464	0.482	0.476	0.471	0.463	0.472	0.465
ETTh2	96	0.327	0.366	0.335	0.367	0.346	0.391	0.332	0.366	0.332	0.371	0.333	0.366	0.338	0.372	0.334	0.369	0.336	0.370	0.338	0.369
	192	0.401	0.410	0.408	0.411	0.415	0.429	0.404	0.409	0.403	0.412	0.406	0.410	0.410	0.414	0.405	0.410	0.407	0.412	0.412	0.413
	336	0.433	0.440	0.443	0.441	0.443	0.453	0.439	0.439	0.437	0.441	0.443	0.442	0.442	0.443	0.438	0.439	0.441	0.442	0.447	0.443
	720	0.420	0.444	0.429	0.445	0.442	0.462	0.428	0.444	0.431	0.448	0.434	0.448	0.430	0.445	0.425	0.443	0.431	0.446	0.433	0.447
	Avg	0.395	0.415	0.404	0.416	0.411	0.433	0.401	0.415	0.401	0.423	0.404	0.416	0.405	0.419	0.401	0.415	0.408	0.418	0.408	0.418
ETTh3	96	0.403	0.417	0.417	0.417	0.417	0.414	0.420	0.416	0.415	0.417	0.411	0.416	0.415	0.418	0.412	0.414	0.412	0.414	0.421	0.419
	192	0.443	0.436	0.460	0.440	0.460	0.448	0.460	0.457	0.460	0.457	0.447	0.440	0.460	0.440	0.459	0.442	0.457	0.438	0.464	0.441
	336	0.494	0.462	0.515	0.469	0.488	0.466	0.505	0.461	0.485	0.450	0.515	0.471	0.516	0.470	0.515	0.472	0.515	0.469	0.521	0.472
	720	0.592	0.508	0.617	0.517	0.557	0.508	0.632	0.464	0.534	0.474	0.625	0.520	0.620	0.518	0.621	0.522	0.623	0.519	0.625	0.520
	Avg	0.483	0.456	0.502	0.461	0.481	0.459	0.503	0.450	0.474	0.456	0.502	0.462	0.502	0.461	0.503	0.463	0.502	0.460	0.508	0.463
ETTm2	96	0.192	0.270	0.191	0.270	0.194	0.283	0.188	0.270	0.191	0.278	0.192	0.274	0.198	0.283	0.192	0.271	0.190	0.271	0.193	0.269
	192	0.258	0.309	0.255	0.310	0.255	0.318	0.248	0.308	0.255	0.316	0.255	0.313	0.261	0.319	0.256	0.310	0.254	0.311	0.259	0.310
	336	0.321	0.350	0.317	0.351	0.315	0.356	0.307	0.346	0.313	0.355	0.317	0.352	0.323	0.358	0.318	0.350	0.316	0.352	0.323	0.351
	720	0.427	0.412	0.420	0.412	0.415	0.414	0.408	0.406	0.414	0.414	0.420	0.412	0.422	0.415	0.418	0.409	0.421	0.413	0.428	0.412
	Avg	0.300	0.335	0.296	0.335	0.325	0.342	0.313	0.333	0.318	0.341	0.322	0.339	0.326	0.344	0.321	0.335	0.320	0.337	0.301	0.336
Traffic	96	0.646	0.358	0.643	0.357	N/A	N/A	N/A	N/A	N/A	N/A	0.642	0.356	0.642	0.357	0.647	0.361	0.646	0.360	0.647	0.361
	192	0.650	0.366	0.654	0.364	N/A	N/A	N/A	N/A	N/A	N/A	0.652	0.365	0.652	0.366	0.659	0.371	0.654	0.367	0.659	0.371
	336	0.670	0.388	0.681	0.388	N/A	N/A	N/A	N/A	N/A	N/A	0.679	0.386	0.679	0.388	0.689	0.395	0.684	0.388	0.689	0.395
	720	0.782	0.462	0.801	0.462	N/A	N/A	N/A	N/A	N/A	N/A	0.792	0.457	0.792	0.462	0.813	0.470	0.801	0.460	0.812	0.470
	Avg	0.687	0.394	0.720	0.418	N/A	N/A	N/A	N/A	N/A	N/A	0.691	0.391	0.691	0.393	0.702	0.414	0.733	0.417	0.702	0.399
Weather	96	0.187	0.234	0.187	0.237	0.184	0.240	0.196	0.245	0.203	0.240	0.214	0.254	0.199	0.246	0.188	0.237	0.202	0.247	0.188	0.236
	192	0.232	0.271	0.232	0.273	0.227	0.274	0.239	0.280	0.240	0.276	0.252	0.286	0.239	0.279	0.233	0.274	0.240	0.276	0.235	0.275
	336	0.284	0.308	0.283	0.310	0.275	0.307	0.289	0.315	0.281	0.310	0.295	0.318	0.286	0.314	0.285	0.310	0.282	0.310	0.289	0.312
	720	0.367	0.362	0.367	0.363	0.353	0.358	0.362	0.367	0.349	0.361	0.368	0.361	0.363	0.369	0.364	0.349	0.361	0.375	0.367	
	Avg	0.268	0.294	0.267	0.308	0.260	0.310	0.287	0.327	0.268	0.322	0.332	0.331	0.311	0.325	0.319	0.309	0.268	0.308	0.270	0.296
Electricity	96	0.167	0.271	0.168	0.272	N/A	N/A	N/A	N/A	N/A	N/A	0.168	0.272	0.166	0.270	0.167	0.272	0.168	0.272	0.168	0.271
	192	0.183	0.284	0.184	0.285	N/A	N/A	N/A	N/A	N/A	N/A	0.184	0.285	0.182	0.284	0.183	0.285	0.184	0.285	0.184	0.285
	336	0.202	0.303	0.204	0.304	N/A	N/A	N/A	N/A	N/A	N/A	0.204	0.304	0.201	0.303	0.203	0.304	0.204	0.304	0.203	0.304
	720	0.254	0.344	0.257	0.347	N/A	N/A	N/A	N/A	N/A	N/A	0.257	0.347	0.252	0.343	0.256	0.344	0.257	0.347	0.256	0.347
	Avg	0.202	0.301	0.203	0.302	N/A	N/A	N/A	N/A	N/A	N/A	0.203	0.302	0.201	0.300	0.202	0.301	0.203	0.302	0.203	0.302
Total	Best	3	3	1	0	1	0	0	3	1	0	0	1	1	1	1	0	1	0	0	0
	Second Best	2	3	1	2	1	0	1	0	2	2	1	1	1	1	1	0	1	0	0	0
	Total	5	6	2	2	2	0	1	3	3	2	1	2	2	2	1	2	0	0	0	1

918
919
920
921
922
923
924
925
926
927
928
929
930

931 Table 6: Raw MSE and MAE results using TimeXer as the backbone forecaster across multiple
932 datasets and horizons. Lower values are better. Red denotes the best value and blue is the second
933 best.

Dataset	STD (Ours)		MLP		Logistic		RF		XGB		LSTM		GRU		CNN		TF		TimeXer			
	MSE	MAE	MSE	MAE	MSE	MAE	MSE	MAE	MSE	MAE	MSE	MAE	MSE	MAE	MSE	MAE	MSE	MAE	MSE	MAE		
ETTh1	96	0.394	0.418	0.397	0.407	0.492	0.417	0.401	0.409	0.408	0.410	0.405	0.419	0.431	0.421	0.400	0.415	0.399	0.417	0.395	0.407	
	192	0.441	0.449	0.447	0.438	0.534	0.449	0.449	0.442	0.456	0.443	0.452	0.450	0.487	0.455	0.447	0.447	0.445	0.446	0.447	0.441	
	336	0.489	0.481	0.494	0.469	0.583	0.483	0.497	0.474	0.504	0.475	0.502	0.482	0.543	0.488	0.501	0.482	0.493	0.476	0.500	0.474	
	720	0.556	0.533	0.543	0.519	0.662	0.535	0.548	0.520	0.561	0.523	0.560	0.531	0.628	0.546	0.573	0.538	0.554	0.524	0.557	0.524	
	Avg	0.470	0.470	0.470	0.458	0.568	0.471	0.474	0.461	0.482	0.463	0.480	0.470	0.522	0.478	0.480	0.468	0.470	0.466	0.475	0.462	
ETTh2	96	0.290	0.343	0.294	0.346	0.324	0.397	0.291	0.346	0.293	0.350	0.293	0.345	0.292	0.343	0.292	0.343	0.292	0.344	0.293	0.344	
	192	0.374	0.394	0.381	0.399	0.405	0.443	0.375	0.397	0.378	0.402	0.380	0.399	0.377	0.397	0.378	0.396	0.375	0.395	0.379	0.397	
	336	0.421	0.433	0.430	0.439	0.447	0.475	0.423	0.435	0.428	0.441	0.430	0.437	0.426	0.436	0.426	0.435	0.421	0.434	0.428	0.436	
	720	0.439	0.453	0.449	0.459	0.482	0.499	0.441	0.455	0.451	0.464	0.446	0.457	0.445	0.457	0.442	0.454	0.438	0.454	0.445	0.456	
	Avg	0.381	0.406	0.388	0.411	0.414	0.454	0.383	0.408	0.387	0.414	0.387	0.409	0.385	0.409	0.384	0.407	0.381	0.407	0.386	0.408	
ETTh3	96	0.313	0.357	0.319	0.360	0.314	0.357	0.318	0.359	0.316	0.361	0.321	0.360	0.321	0.360	0.320	0.361	0.320	0.360	0.322	0.361	
	192	0.367	0.391	0.382	0.399	0.375	0.395	0.380	0.397	0.378	0.399	0.385	0.399	0.384	0.399	0.383	0.400	0.383	0.399	0.385	0.400	
	336	0.421	0.425	0.445	0.437	0.436	0.433	0.442	0.435	0.445	0.438	0.448	0.437	0.446	0.437	0.446	0.446	0.438	0.445	0.436	0.449	0.438
	720	0.524	0.481	0.558	0.496	0.547	0.491	0.554	0.493	0.559	0.494	0.562	0.496	0.560	0.495	0.560	0.497	0.559	0.494	0.563	0.497	
	Avg	0.406	0.414	0.426	0.423	0.418	0.419	0.424	0.421	0.424	0.423	0.429	0.423	0.428	0.423	0.427	0.424	0.427	0.422	0.411	0.424	
ETTM2	96	0.169	0.267	0.172	0.259	0.171	0.266	0.170	0.258	0.172	0.265	0.185	0.267	0.173	0.261	0.181	0.271	0.191	0.262	0.174	0.259	
	192	0.232	0.308	0.237	0.303	0.233	0.306	0.232	0.301	0.235	0.307	0.234	0.308	0.230	0.304	0.247	0.315	0.251	0.305	0.241	0.304	
	336	0.299	0.349	0.304	0.347	0.299	0.347	0.298	0.343	0.300	0.348	0.287	0.349	0.307	0.347	0.314	0.357	0.308	0.347	0.311	0.348	
	720	0.408	0.410	0.410	0.410	0.401	0.407	0.403	0.405	0.404	0.409	0.585	0.519	0.414	0.409	0.414	0.415	0.406	0.408	0.421	0.411	
	Avg	0.277	0.334	0.281	0.330	0.276	0.332	0.276	0.327	0.278	0.332	0.473	0.458	0.283	0.330	0.289	0.339	0.287	0.331	0.287	0.331	
Traffic	96	0.468	0.301	0.469	0.300	N/A	N/A	N/A	N/A	N/A	N/A	0.467	0.298	0.468	0.298	0.471	0.299	0.471	0.300	0.471	0.303	
	192	0.471	0.302	0.471	0.300	N/A	N/A	N/A	N/A	N/A	N/A	0.469	0.298	0.470	0.299	0.473	0.299	0.473	0.300	0.473	0.303	
	336	0.470	0.300	0.470	0.298	N/A	N/A	N/A	N/A	N/A	N/A	0.468	0.296	0.469	0.297	0.473	0.298	0.473	0.298	0.473	0.301	
	720	0.476	0.302	0.477	0.300	N/A	N/A	N/A	N/A	N/A	N/A	0.475	0.298	0.475	0.299	0.479	0.300	0.479	0.301	0.479	0.303	
	Avg	0.471	0.301	0.472	0.300	N/A	N/A	N/A	N/A	N/A	N/A	0.470	0.298	0.471	0.298	0.474	0.299	0.474	0.300	0.474	0.303	
Weather	96	0.159	0.207	0.162	0.217	0.159	0.218	0.159	0.210	0.158	0.216	0.160	0.209	0.161	0.209	0.160	0.209	0.160	0.209	0.161	0.207	
	192	0.205	0.248	0.208	0.257	0.203	0.257	0.206	0.252	0.203	0.256	0.207	0.251	0.206	0.251	0.207	0.252	0.206	0.252	0.209	0.250	
	336	0.260	0.289	0.262	0.296	0.256	0.294	0.261	0.292	0.257	0.296	0.262	0.291	0.262	0.291	0.263	0.292	0.261	0.292	0.265	0.292	
	720	0.338	0.340	0.341	0.346	0.333	0.344	0.340	0.343	0.334	0.346	0.340	0.342	0.342	0.343	0.344	0.344	0.340	0.344	0.348	0.345	
	Avg	0.241	0.271	0.243	0.279	0.238	0.278	0.242	0.274	0.238	0.279	0.242	0.273	0.242	0.273	0.243	0.274	0.242	0.274	0.246	0.274	
Electricity	96	0.139	0.240	0.140	0.241	N/A	N/A	N/A	N/A	N/A	N/A	0.139	0.240	0.140	0.241	0.140	0.241	0.139	0.239	0.140	0.242	
	192	0.165	0.266	0.167	0.271	N/A	N/A	N/A	N/A	N/A	N/A	0.166	0.269	0.167	0.270	0.167	0.270	0.164	0.266	0.167	0.271	
	336	0.200	0.303	0.205	0.310	N/A	N/A	N/A	N/A	N/A	N/A	0.202	0.307	0.204	0.309	0.205	0.309	0.199	0.303	0.204	0.311	
	720	0.294	0.385	0.304	0.394	N/A	N/A	N/A	N/A	N/A	N/A	0.298	0.390	0.303	0.394	0.304	0.394	0.294	0.385	0.304	0.395	
	Avg	0.200	0.298	0.204	0.304	N/A	N/A	N/A	N/A	N/A	N/A	0.201	0.302	0.204	0.304	0.204	0.304	0.199	0.298	0.203	0.302	
Total	Best	3	4	1	1	2	0	1	1	1	0	1	1	0	1	0	0	2	1	0	0	
	Second Best	4	0	0	1	0	1	1	0	0	0	0	2	1	2	1	1	1	1	1	1	
	Total	7	4	1	2	2	1	2	2	1	0	1	3	1	3	0	2	3	2	1	1	

972
973
974
975
976
977
978
979
980
981
982
983
984

985 Table 7: Raw MSE and MAE results using TimeBridge as the backbone forecaster across multiple
986 datasets and horizons. Lower values are better. Red denotes the best value and blue is the second
987 best.

988	Dataset	STD (Ours)		MLP		Logistic		RF		XGB		LSTM		GRU		CNN		TF		TimeBridge		
		MSE	MAE																			
989	ETTh1	96	0.382	0.404	0.385	0.402	0.388	0.405	0.388	0.402	0.388	0.416	0.435	0.447	0.387	0.413	0.390	0.410	0.389	0.413	0.385	0.401
		192	0.429	0.433	0.432	0.429	0.435	0.434	0.435	0.430	0.435	0.443	0.487	0.473	0.435	0.440	0.438	0.440	0.436	0.439	0.434	0.431
		336	0.469	0.456	0.471	0.451	0.477	0.458	0.476	0.452	0.475	0.465	0.536	0.498	0.479	0.466	0.481	0.465	0.479	0.462	0.478	0.456
		720	0.495	0.485	0.492	0.481	0.508	0.491	0.492	0.478	0.496	0.490	0.548	0.520	0.514	0.501	0.510	0.502	0.506	0.494	0.499	0.487
		Avg	0.444	0.444	0.445	0.441	0.452	0.447	0.448	0.441	0.449	0.454	0.502	0.485	0.454	0.455	0.455	0.454	0.453	0.452	0.449	0.444
990	ETTh2	96	0.296	0.346	0.301	0.350	0.322	0.395	0.298	0.351	0.300	0.354	0.298	0.348	0.297	0.348	0.298	0.349	0.296	0.351	0.300	0.348
		192	0.379	0.396	0.385	0.401	0.400	0.440	0.380	0.400	0.381	0.404	0.380	0.399	0.380	0.398	0.378	0.398	0.375	0.400	0.383	0.399
		336	0.431	0.436	0.437	0.441	0.446	0.473	0.431	0.438	0.432	0.442	0.430	0.438	0.432	0.438	0.428	0.437	0.425	0.438	0.435	0.439
		720	0.444	0.454	0.454	0.461	0.478	0.495	0.444	0.456	0.453	0.463	0.444	0.456	0.449	0.458	0.444	0.455	0.446	0.458	0.448	0.456
		Avg	0.388	0.408	0.394	0.413	0.411	0.451	0.388	0.411	0.391	0.416	0.388	0.410	0.390	0.411	0.387	0.410	0.386	0.412	0.392	0.411
991	ETTm1	96	0.320	0.360	0.322	0.363	0.320	0.361	0.324	0.362	0.320	0.362	0.326	0.371	0.326	0.364	0.333	0.374	0.324	0.362	0.325	0.363
		192	0.375	0.394	0.377	0.397	0.375	0.395	0.379	0.397	0.374	0.395	0.383	0.398	0.383	0.399	0.392	0.409	0.381	0.397	0.382	0.398
		336	0.424	0.426	0.427	0.427	0.424	0.426	0.429	0.428	0.422	0.426	0.432	0.435	0.433	0.430	0.450	0.442	0.432	0.429	0.433	0.430
		720	0.521	0.474	0.523	0.474	0.519	0.473	0.527	0.476	0.516	0.472	0.531	0.478	0.531	0.478	0.558	0.490	0.530	0.477	0.532	0.478
		Avg	0.410	0.414	0.412	0.415	0.409	0.414	0.415	0.416	0.408	0.414	0.418	0.420	0.419	0.418	0.433	0.429	0.417	0.416	0.418	0.417
992	ETTm2	96	0.179	0.260	0.180	0.263	0.180	0.271	0.177	0.283	0.180	0.270	0.183	0.268	0.183	0.267	0.180	0.262	0.184	0.338	0.181	0.262
		192	0.245	0.304	0.246	0.306	0.241	0.310	0.239	0.319	0.241	0.310	0.247	0.310	0.247	0.310	0.246	0.305	0.246	0.373	0.248	0.305
		336	0.311	0.346	0.314	0.347	0.303	0.349	0.300	0.353	0.301	0.349	0.312	0.350	0.311	0.349	0.311	0.346	0.308	0.406	0.398	0.409
		720	0.418	0.407	0.419	0.408	0.404	0.407	0.403	0.408	0.404	0.409	0.416	0.409	0.417	0.409	0.418	0.407	0.414	0.459	0.422	0.408
		Avg	0.288	0.329	0.290	0.331	0.282	0.334	0.280	0.341	0.282	0.335	0.289	0.335	0.289	0.334	0.289	0.330	0.288	0.394	0.312	0.346
993	Traffic	96	0.534	0.358	0.553	0.369	N/A	N/A	N/A	N/A	N/A	N/A	0.544	0.362	0.545	0.362	0.553	0.369	0.553	0.369	0.553	0.369
		192	0.579	0.375	0.595	0.385	N/A	N/A	N/A	N/A	N/A	N/A	0.584	0.377	0.584	0.377	0.595	0.385	0.595	0.385	0.594	0.385
		336	0.654	0.397	0.664	0.405	N/A	N/A	N/A	N/A	N/A	N/A	0.650	0.396	0.651	0.397	0.664	0.405	0.664	0.405	0.664	0.405
		720	0.805	0.450	0.813	0.456	N/A	N/A	N/A	N/A	N/A	N/A	0.796	0.447	0.798	0.448	0.813	0.456	0.796	0.450	0.811	0.456
		Avg	0.643	0.395	0.656	0.404	N/A	N/A	N/A	N/A	N/A	N/A	0.644	0.396	0.645	0.396	0.656	0.404	0.652	0.402	0.656	0.404
994	Weather	96	0.159	0.208	0.160	0.211	0.160	0.220	0.161	0.211	0.160	0.219	0.160	0.210	0.161	0.210	0.161	0.209	0.160	0.210	0.162	0.209
		192	0.205	0.249	0.203	0.250	0.203	0.257	0.205	0.252	0.211	0.271	0.205	0.251	0.207	0.251	0.206	0.250	0.204	0.251	0.208	0.250
		336	0.259	0.290	0.256	0.288	0.254	0.294	0.259	0.291	0.262	0.307	0.259	0.290	0.262	0.291	0.261	0.290	0.257	0.291	0.263	0.291
		720	0.340	0.342	0.336	0.338	0.330	0.341	0.337	0.341	0.335	0.353	0.337	0.340	0.341	0.342	0.340	0.340	0.335	0.340	0.345	0.343
		Avg	0.241	0.272	0.239	0.272	0.237	0.278	0.241	0.274	0.242	0.288	0.240	0.273	0.243	0.274	0.242	0.275	0.239	0.273	0.245	0.273
995	Electricity	96	0.195	0.282	0.195	0.281	N/A	N/A	N/A	N/A	N/A	N/A	0.194	0.280	0.195	0.281	0.195	0.282	0.194	0.280	0.195	0.282
		192	0.214	0.299	0.214	0.299	N/A	N/A	N/A	N/A	N/A	N/A	0.213	0.297	0.214	0.298	0.214	0.299	0.213	0.298	0.214	0.299
		336	0.240	0.322	0.240	0.322	N/A	N/A	N/A	N/A	N/A	N/A	0.238	0.320	0.239	0.321	0.240	0.322	0.238	0.320	0.240	0.322
		720	0.296	0.368	0.296	0.366	N/A	N/A	N/A	N/A	N/A	N/A	0.293	0.363	0.295	0.365	0.296	0.366	0.294	0.364	0.295	0.366
		Avg	0.236	0.318	0.236	0.317	N/A	N/A	N/A	N/A	N/A	N/A	0.235	0.315	0.236	0.316	0.236	0.317	0.235	0.316	0.236	0.317
996	Second Best	2	5	0	2	1	1	1	1	1	1	1	1	0	0	0	0	2	0	0	0	
		1	1	3	1	2	0	0	0	0	1	1	3	1	1	2	2	2	0	2	1	
		Total	3	6	3	3	1	1	1	1	2	4	1	2	2	2	2	2	2	1	2	

1014
1015
1016
1017
1018
1019
1020
1021
1022
1023
1024
1025

1026

1027 Table 8: Average Error Reduction in MSE compared to TimeBridge for different UEC methods (the
 1028 lower the better, negative means improvement). N/A indicates that the method failed to converge or
 1029 crashed during training. Bold and underline denote best and second-best results, respectively.

Method	ETTh1	ETTh2	ETTm1	ETTm2	Traffic	Weather	Electricity
AR (No Correction)	0.00	0.00	0.00	0.00	0.00	0.00	0.00
UEC-MLP	-0.84	0.69	-1.35	-7.24	0.09	-2.26	-0.03
UEC-Logistic	0.67	5.08	-2.06	-9.65	N/A	-3.07	N/A
UEC-Random Forest	-0.21	-0.84	-0.83	-10.4	N/A	-1.61	N/A
UEC-XGBoost	-0.10	-0.06	-2.41	<u>-9.81</u>	N/A	-0.87	N/A
UEC-LSTM	11.6	-0.86	-0.01	-7.33	<u>-1.82</u>	-1.60	-0.64
UEC-GRU	1.08	-0.51	0.10	-7.29	-1.65	-0.62	-0.21
UEC-CNN	1.31	<u>-1.17</u>	3.64	-7.57	0.09	-0.92	0.05
UEC-Transformer	0.80	-1.49	-0.28	-7.78	-0.54	-2.19	<u>-0.61</u>
UEC-STD	-1.15	-1.03	-1.92	-7.63	-1.91	-1.43	0.02

1040

1041

1042 Table 9: Average Error Reduction in MAE compared to TimeBridge for different UEC methods (the
 1043 lower the better, negative means improvement). N/A indicates that the method failed to converge or
 1044 crashed during training. Bold and underline denote best and second-best results, respectively.

Method	ETTh1	ETTh2	ETTm1	ETTm2	Traffic	Weather	Electricity
AR (No Correction)	0.00	0.00	0.00	0.00	0.00	0.00	0.00
UEC-MLP	-0.77	0.66	-0.57	-4.36	-0.01	-0.40	-0.09
UEC-Logistic	0.70	9.76	<u>-0.90</u>	-3.29	N/A	1.77	N/A
UEC-Random Forest	-0.81	0.21	-0.41	-1.54	N/A	0.25	N/A
UEC-XGBoost	2.19	1.26	-0.83	-3.25	N/A	5.39	N/A
UEC-LSTM	9.15	-0.07	0.73	-3.27	<u>-1.98</u>	-0.21	-0.60
UEC-GRU	2.49	0.03	0.05	-3.50	-1.86	0.18	-0.20
UEC-CNN	2.32	<u>-0.21</u>	2.73	<u>-4.58</u>	-0.01	-0.21	0.01
UEC-Transformer	1.85	0.32	-0.26	13.9	-0.36	0.02	<u>-0.52</u>
UEC-STD	0.13	-0.61	-0.92	-4.82	-2.13	-0.40	-0.08

1055

1056

C.4 HYPERPARAMETERS

1058

1059

C.4.1 HYPERPARAMETERS OF BACKBONES

1060

1061

The hyperparameters for the backbone models (TimeMixer, TimesNet, and TimeXer) are adopted directly from the official Time-Series-Library repository by THUML², in line with their experimental settings. These settings (such as look-back length, model depth, hidden sizes, and other architecture-specific parameters) are consistent with those used in the TSLib implementation. At the same time, some hyperparameters are dataset-dependent, meaning that choices like sequence length, batch size, or certain regularization parameters vary depending on the particular dataset in use.

1066

1067

C.4.2 HYPERPARAMETERS OF UEC

1068

1069

1070

1071

1072

1073

1074

All UEC models in our experiments were trained using the same set of hyperparameters summarized in Table 10. The same set of corrections was constructed from the validation split \mathcal{D}_{val} , with a 70/30 split for training and early stopping / β tuning, was used for all UEC models. The correction strength β was selected separately for MSE and MAE using a balanced validation strategy, and it is reported in Table 11. Based on the results in Table 14, we chose the Huber loss to train all UEC models, as it consistently led to the best performance across both MSE and MAE metrics.

1075

1076

1077

1078

1079

²<https://github.com/thuml/Time-Series-Library>

1080
1081
1082
1083
1084
1085
1086
1087
1088
1089
1090
1091
1092
1093
1094
1095
1096
1097
1098
1099
1100
1101
1102
1103
1104
1105
1106
1107
1108
1109
1110
1111
1112
1113
1114
1115
1116
1117
1118
1119
1120
1121
1122
1123
1124
1125
1126
1127
1128
1129
1130
1131
1132
1133

Table 10: Default Training Parameters of UEC

Parameter	Value / Description
Correction data	$\mathcal{U}_{\text{train}} / \mathcal{U}_{\text{val}}$ (70%/30%) from \mathcal{D}_{val}
Training procedure	Follows Sect. 2.2 and Sect. 2.3
Number of training steps	100
Batch size	64
Loss	Huber (HL) Loss
Correction strength β	Selected separately for MSE and MAE refer to Table 11

C.5 DETAILS ON MODEL ANALYSIS

Table 13 compares the averaged MSE and MAE of direct forecasting (DF) and autoregressive (AR) methods across models, showing that AR consistently outperforms DF.

Figure 4 provides qualitative examples on the TRAFFIC dataset, illustrating how UEC mitigates collapse by restoring variance and correcting drift.

Table 14 presents the impact of different training losses on UEC performance for ETTh1, indicating Huber loss often yields the best results.

Figure 6 demonstrates performance improvements of UEC-enhanced backbones across multiple prediction lengths, highlighting consistent gains over standard backbone predictions.

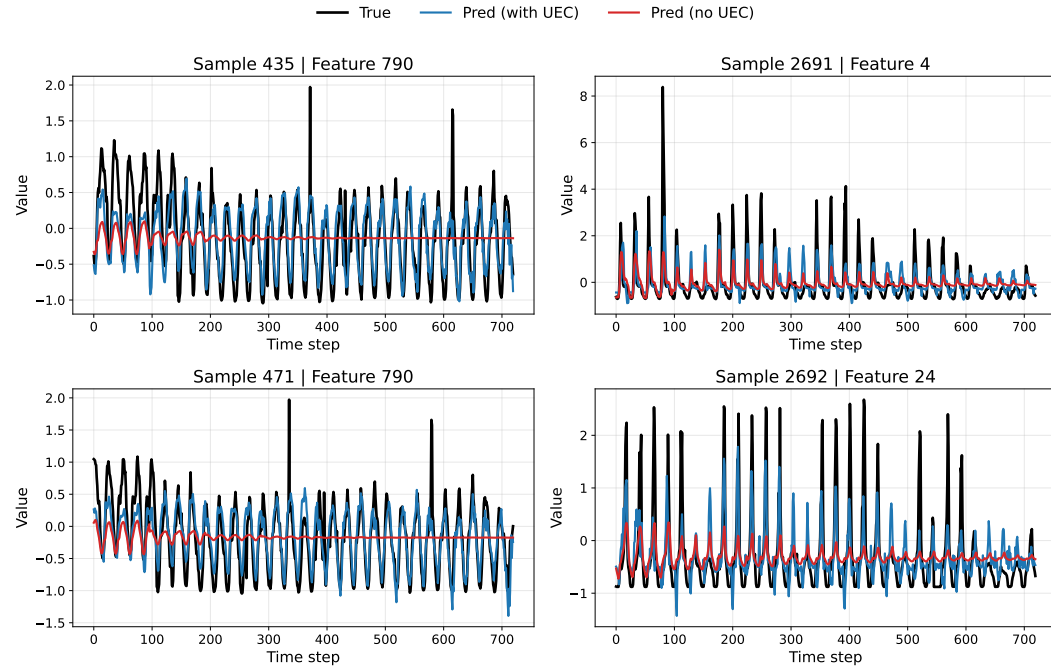


Figure 4: Qualitative examples on TRAFFIC using TimesNet as backbone model (prediction length = 720). Each panel shows the ground truth, prediction with UEC, and prediction without UEC. UEC mitigates collapse by restoring variance and correcting drift.

C.6 KERNEL SIZE SENSITIVITY ANALYSIS

1134
1135
1136
1137
1138
1139
1140
1141
1142
1143
1144
1145
1146
1147
1148
1149
1150

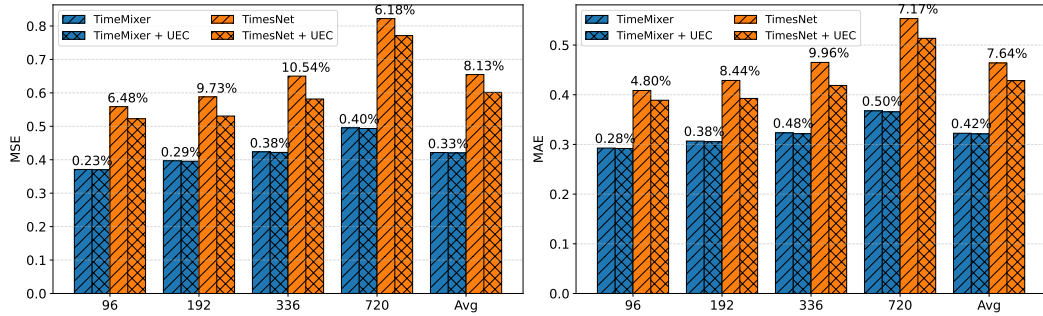


Figure 5: Performance of extended training across different prediction lengths: 96, 192, 336, and 720. Backbone models (TimeMixer and TimesNet) are compared with their corresponding UEC-enhanced versions. % improvement is annotated on top of each bar pair.

1154
1155
1156
1157
1158
1159
1160
1161
1162
1163
1164
1165
1166
1167
1168
1169
1170
1171
1172
1173
1174
1175
1176
1177
1178
1179
1180
1181
1182
1183
1184
1185
1186
1187

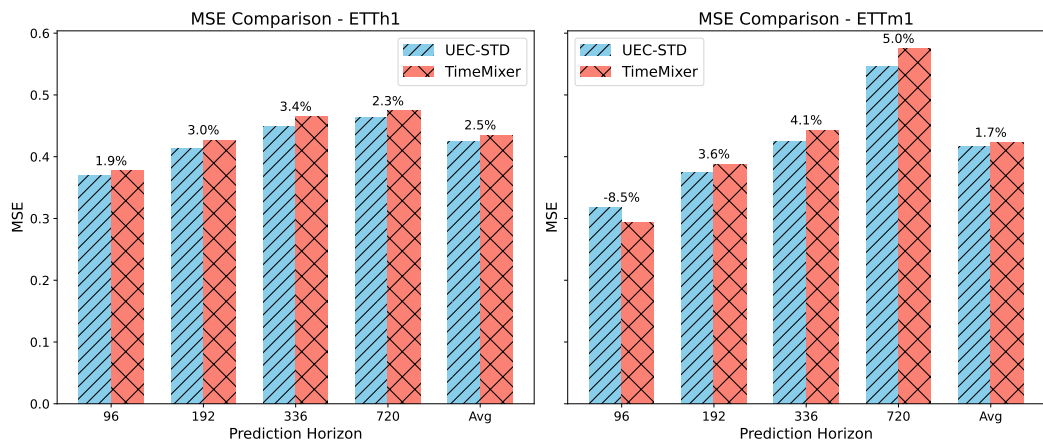


Figure 6: Performance across different prediction lengths: 96, 192, 336, and 720. TimeMixer is compared with its corresponding UEC-enhanced versions on ETTh1 and ETTm1 datasets. % improvement is annotated on top of each bar pair.

1188
1189
1190
1191
1192
1193

1194 Table 11: Found Correction Strength β for UEC Models Across Datasets and Backbones

Dataset	Backbone	STD (Ours)		MLP		Logistic		RF		XGB		LSTM		GRU		CNN		TF.	
		MSE	MAE	MSE	MAE	MSE	MAE	MSE	MAE	MSE	MAE	MSE	MAE	MSE	MAE	MSE	MAE	MSE	MAE
ETTh1	TimeXer	0.3	0.3	0.7	0.5	0.1	0.1	0.7	0.3	0.3	0.1	0.3	0.3	0.3	0.5	0.3	0.5	0.3	0.3
	TimeNet	0.5	0.3	0.5	0.3	0.3	0.3	0.7	0.3	0.3	0.1	0.3	0.3	0.3	0.5	0.3	0.1	0.3	0.5
	TimeBridge	0.3	0.3	0.1	0.3	0.3	0.3	0.5	0.1	0.3	0.1	0.3	0.3	0.3	0.5	0.3	0.1	0.3	0.3
	TimeMixer	0.3	0.3	0.3	0.3	0.1	0.1	0.5	0.3	0.3	0.3	0.3	0.3	0.3	0.5	0.3	0.3	0.3	0.3
ETTh2	TimeXer	0.1	0.1	0.1	0.1	0.1	0.1	0.1	0.1	0.1	0.1	0.1	0.1	0.1	0.1	0.1	0.1	0.1	0.1
	TimeNet	0.1	0.1	0.1	0.1	0.1	0.1	0.1	0.1	0.1	0.1	0.1	0.1	0.1	0.1	0.1	0.1	0.1	0.1
	TimeBridge	0.1	0.1	0.1	0.1	0.1	0.1	0.1	0.1	0.1	0.1	0.1	0.1	0.1	0.1	0.1	0.1	0.3	0.1
	TimeMixer	0.1	0.1	0.1	0.1	0.1	0.1	0.1	0.1	0.1	0.1	0.1	0.1	0.1	0.1	0.1	0.1	0.1	0.1
ETTm1	TimeXer	0.3	0.5	0.1	0.3	0.1	0.1	0.1	0.1	0.1	0.1	0.1	0.3	0.1	0.3	0.1	0.3	0.1	0.1
	TimeNet	0.3	0.5	0.1	0.1	0.3	0.1	0.1	0.1	0.1	0.1	0.1	0.1	0.3	0.1	0.1	0.1	0.1	0.1
	TimeBridge	0.5	0.5	0.1	0.1	0.1	0.1	0.1	0.1	0.1	0.1	0.1	0.1	0.1	0.1	0.1	0.1	0.3	0.1
	TimeMixer	0.5	0.7	0.3	0.3	0.1	0.1	0.1	0.1	0.1	0.1	0.1	0.3	0.1	0.1	0.1	0.3	0.1	0.1
ETTm2	TimeXer	0.1	0.3	0.1	0.1	0.1	0.1	0.1	0.1	0.1	0.1	0.1	0.3	0.1	0.3	0.1	0.3	0.1	0.1
	TimeNet	0.1	0.1	0.3	0.1	0.1	0.1	0.1	0.1	0.1	0.1	0.1	0.1	0.1	0.1	0.1	0.1	0.1	0.1
	TimeBridge	0.3	0.3	0.5	0.3	0.1	0.1	0.1	0.1	0.1	0.1	0.1	0.1	0.1	0.1	0.1	0.1	0.1	0.3
	TimeMixer	0.1	0.1	0.1	0.1	0.1	0.1	0.1	0.3	0.1	0.1	0.1	0.1	0.1	0.1	0.1	0.1	0.1	0.3

1237
1238
1239
1240
1241

1242

1243

1244

1245

1246

1247

Table 12: Found Correction Strength β for UEC Models Across Datasets and Backbones (cont.)

Dataset	Backbone	STD (Ours)		MLP		Logistic		RF		XGB		LSTM		GRU		CNN		TF	
		MSE	MAE	MSE	MAE	MSE	MAE	MSE	MAE	MSE	MAE	MSE	MAE	MSE	MAE	MSE	MAE	MSE	MAE
Traffic	Traffic	0.1	0.1	0.1	0.1	N/A	N/A	N/A	N/A	N/A	N/A	0.1	0.1	0.1	0.1	0.1	0.3	0.3	0.1
	TimeBridge	0.3	0.1	0.1	0.1	N/A	N/A	N/A	N/A	N/A	N/A	0.1	0.1	0.1	0.1	0.1	0.1	0.1	0.1
	TimeXer	0.1	0.5	0.1	0.1	N/A	N/A	N/A	N/A	N/A	N/A	0.1	0.1	0.1	0.1	0.1	1.0	0.1	1.0
	TimeNet	0.1	0.1	0.1	0.1	0.1	0.1	0.1	0.3	0.1	0.1	0.1	0.1	0.1	0.1	0.1	0.1	0.1	0.3
Weather	Weather	0.1	0.1	0.1	0.1	0.1	0.1	0.1	0.1	0.1	0.1	0.3	0.1	0.3	0.3	0.1	0.1	0.3	0.1
	TimeBridge	0.1	0.1	0.1	0.1	0.1	0.1	0.5	0.1	0.3	0.1	0.5	0.3	0.5	0.3	0.1	0.1	0.3	0.3
	TimeXer	0.1	0.1	0.1	0.1	0.1	0.1	0.1	0.1	0.1	0.1	0.1	0.1	0.1	0.1	0.1	0.1	0.1	0.1
	TimeNet	0.1	0.1	0.1	0.1	0.1	0.1	0.1	0.1	0.1	0.1	0.1	0.1	0.1	0.1	0.1	0.1	0.1	0.1
Electricity	Electricity	0.1	0.1	0.3	0.1	N/A	N/A	N/A	N/A	N/A	N/A	0.1	0.1	0.1	0.1	0.1	0.1	0.1	0.1
	TimeBridge	0.3	0.1	0.1	0.1	N/A	N/A	N/A	N/A	N/A	N/A	0.1	0.1	0.1	0.1	0.1	0.1	0.1	0.1
	TimeXer	0.1	0.1	0.1	0.3	N/A	N/A	N/A	N/A	N/A	N/A	0.1	0.1	0.1	0.1	0.1	1.0	0.1	1.0
	TimeNet	0.1	0.1	0.1	0.1	0.1	0.1	0.1	0.1	0.1	0.1	0.1	0.1	0.1	0.1	0.1	0.1	0.1	0.1

1276

1277

1278

1279

Table 13: Performance comparison (averaged MSE and MAE across prediction lengths 96, 192, 336, and 720) for AR and DF methods on different datasets and models.

Dataset	Model	DF (MSE / MAE)	AR (MSE / MAE)
ETTh1	TimeMixer	0.4490 / 0.4399	0.4357 / 0.4348
ETTh1	TimesNet	0.4879 / 0.4722	0.4715 / 0.4655
Weather	TimeMixer	0.2445 / 0.2748	0.2446 / 0.2739
Weather	TimesNet	0.2634 / 0.2910	0.2699 / 0.2964
Traffic	TimeMixer	0.5041 / 0.3241	0.5485 / 0.3385
Traffic	TimesNet	0.7606 / 0.4419	0.7014 / 0.3991

1287

1288

1289

1290

Table 14: Results on ETTh1 dataset with different training losses of UEC across backbones. Bold denotes the best results.

Backbone	Huber		L1		MSE	
	MSE	MAE	MSE	MAE	MSE	MAE
TimeMixer	0.434	0.435	0.434	0.438	0.434	0.438
TimesNet	0.534	0.488	0.536	0.491	0.535	0.490

1296
1297
1298
1299 Table 15: Average MSE and MAE across all prediction lengths {96, 192, 336, 720} for ETTm1
1300 dataset using TimeMixer as backbone, with different kernel sizes {5, 25, 50}.

Kernel size	MSE	MAE
5	0.4060	0.4136
25	0.4048	0.4184
50	0.4044	0.4211

1306
1307
1308
1309
1310
1311 Table 16: Mean and standard deviation of MSE and MAE for UEC-STD and TimeMixer (3 runs).

Method	MSE (mean \pm std)	MAE (mean \pm std)
UEC-STD	0.4273 ± 0.0029	0.4343 ± 0.0012
TimeMixer	0.4357 ± 0.0006	0.4343 ± 0.0006

1317
1318
1319
1320
1321
1322 Table 17: Performance gains (MAPE, %) on ETTh1 and ETTm1.

Method	ETTh1	ETTm1
AR (No Correction)	0.00	0.00
UEC-MLP	-3.61	-0.58
UEC-Logistic	-12.48	-2.09
UEC-Random Forest	7.02	-1.74
UEC-XGBoost	-9.89	-4.42
UEC-LSTM	-9.62	-0.59
UEC-GRU	-10.27	-0.83
UEC-CNN	-8.42	-1.07
UEC-TF	3.04	-1.10
UEC-STD	-21.66	-2.16

1336
1337
1338
1339
1340
1341 Table 18: MSE results on the US_Births dataset for different models and prediction horizons.

Horizon	AR	MLP	Logistic	Random Forest	XGBoost	LSTM	GRU	CNN	TF	STD
96	0.2303	0.2265	0.2149	0.2231	0.2219	0.2187	0.2146	0.2282	0.2185	0.2008
192	0.2662	0.2598	0.2370	0.2514	0.2469	0.2462	0.2428	0.2622	0.2493	0.2273
336	0.2806	0.2732	0.2493	0.2631	0.2583	0.2585	0.2564	0.2734	0.2618	0.2309
720	0.3067	0.2965	0.2541	0.2775	0.2656	0.2759	0.2723	0.3108	0.2788	0.2405
Average	0.2709	0.2640	0.2388	0.2537	0.2481	0.2498	0.2465	0.2686	0.2521	0.2248